MIT Libraries | DSpace@MIT

MIT Open Access Articles

Cost effectiveness of conventionally and solar powered monovalent selective electrodialysis for seawater desalination in greenhouses

The MIT Faculty has made this article openly available. ***Please share*** how this access benefits you. Your story matters.

Citation: Ahdab, Yvana D et al. "Cost effectiveness of conventionally and solar powered monovalent selective electrodialysis for seawater desalination in greenhouses." Applied Energy 301 (November 2021): 117425. © 2021 Elsevier Ltd

As Published: http://dx.doi.org/10.1016/j.apenergy.2021.117425

Publisher: Elsevier BV

Persistent URL: https://hdl.handle.net/1721.1/133046

Version: Original manuscript: author's manuscript prior to formal peer review

Terms of use: Creative Commons Attribution-Noncommercial-Share Alike

Massachusetts Institute of Technology

Cost effectiveness of conventionally and solar powered monovalent selective electrodialysis for seawater desalination in greenhouses

Yvana D. Ahdab[a], Georg Schücking[a], Danyal Rehman[a], John H. Lienhard[a,*]

[a]*Rohsenow Kendall Heat Transfer Laboratory, Massachusetts Institute of Technology, 77 Massachusetts Avenue, Cambridge, MA 02139, United States*

Abstract

Reverse osmosis is the most widely used desalination technology for treating irrigation water. Reverse omsosis removes both monovalent ions detrimental to crops (Na^+, Cl^-) and divalent ions beneficial for crops ($Ca^{2+}, Mg^{2+}, SO_4^{2-}$). Fertilizer must then be added to the desalinated water to reintroduce these nutrients. Unlike reverse osmosis, monovalent selective electrodialysis selectively removes monovalent ions while retaining divalent ions in the desalinated water. This paper investigates the monovalent selectivity and cost effectiveness of the widely-used Neosepta and new Fujifilm monovalent selective electrodialysis membranes in treating seawater for irrigation. Membrane selectivity, limiting current, and resistance are experimentally characterized. These system parameters are inputs to the developed cost model, which determines fertilizer and water savings, as well as operating and capital costs, relative to reverse osmosis; the primary operating cost difference stems from reverse osmosis's significantly lower energy consumption. Given prices of commercially available membranes, monovalent selective electrodialysis costs an average of 30% more than reverse osmosis. At the projected sales price of Fujifilm membranes, which are still under development, monovalent selective electrodialysis costs an average of 10% more than reverse osmosis; if electricity costs are less than 0.08 $/kWh, monovalent selective electrodialysis is on par with reverse osmosis. Regardless of membrane price and electricity cost, solar-powered desalination is only economical if photovoltaic capital costs are significantly reduced to 0.10–0.20 $/kWh. When monovalent selective electrodialysis exceeds reverse osmosis cost, the financial requirements of competitive monovalent selective electrodialysis (e.g., energy consumption, electricity cost, energy source, membrane cost) are evaluated.

Keywords: desalination, selective electrodialysis, seawater, photovoltaic, irrigation, cost analysis

*Corresponding author. lienhard@mit.edu

Y.D. Ahdab, G. Schücking, D. Rehman, and J.H. Lienhard V, "Cost effectiveness of conventional and solar powered monovalent selective electrodialysis for seawater desalination in greenhouses," *Applied Energy*, online 20 July 2021, Vol. 301, eid:117425, 1 November 2021. doi:10.1016/j.apenergy.2021.117425

Nomenclature

Roman Symbols

A	Area, m^2
C	Concentration, $mol \cdot m^{-3}$
D	Diffusion coefficient, $m^2 \cdot s^{-1}$
E	Donnan potential, V
F	Faraday constant, $C \cdot mol^{-1}$
h	Channel height, m
i	Current density, $A \cdot m^{-2}$
I	Current, A
J	Flux, $mol \cdot m^{-2} \cdot s^{-1}$
k	Electrical conductivity, $S \cdot m^{-1}$
L_j	Membrane ion permeability, $m \cdot s^{-1}$
L_w	Membrane water permeability, $s \cdot m^{-1}$
m	Slope
M	Molar mass, $mg \cdot mol^{-1}$
m_j	Ion mass, kg
N_{cp}	Number of cell pairs
P	Permselectivity
Q	Volume flow rate, $m^3 \cdot s^{-1}$
r	Discount rate
$\bar{r}$	Resistance
$\mathrm{Re_D}$	Reynolds number
S	Salinity
Sc	Schmidt number
Sh	Sherwood number
T	Transport number
t_{cu}	Integral counter ion transport number
t	Process time, s
V_{el}	Electrode potential, V
$\dot{V}_{\mathrm{p,day}}$	Product flowrate, m^3/day

$\dot{V}_{\mathrm{p,yr}}$	Product flowrate, m^3/yr
V_{stack}	Stack potential, V
w	Concentration, meq
z	Valence

Greek Symbols

π	Osmotic pressure, bar
σ	Spacer shadow effect

Subscripts

c	Concentrate
cu	Counter ion
d	Diluate
div	Divalent
f	Final
j	Ion species
lim	Limiting
m, mem	membrane
mon	Monovalent
$\mathrm{non-mem}$	Non-membrane
o, i	Initial
r	Rinse
s	Salt
w	Water
yr	Annual

Superscripts

cp	Cell pair

Acronyms

AEM	Anion exchange membrane
AF	Annuity factor
BGW	Brackish groundwater
CapEx	Capital expense, $
CEM	Cation exchange membrane
ED	Electrodialysis
MSED	Monovalent selective electrodialysis

OpEx	Operating expense, $
RO	Reverse osmosis
RR	Recovery ratio
SW	Seawater
TDS	Total dissolved solids, $mg \cdot L^{-1}$

1. Introduction

The dominant user of global water supplies is agriculture (69% of freshwater withdrawals according to [1]). Trends in population growth, resource-demanding consumption, and climate change continue to rapidly increase water demand for food production [2]. Advanced agriculture accounts for over 85% of water demand in coastal arid and semiarid regions, such as in Spain [3] and Israel [4]. Numerous strategies, including smart irrigation systems, water conservation, and infrastructure modernization, have been employed to augment irrigation water supply. Such approaches improve water distribution or use without increasing availability. To expand water supply in coastal arid regions, non-conventional water resources, such as desalination and reuse, are the primary methods.

While brackish groundwater (BGW) has served as the primary desalination feedwater for irrigation, the over-extraction of this resource is limiting its availability around the world. In coastal water-scarce regions, another option for desalination feedwater is seawater (SW) [5]. SW is an abundant resource that does not face the same environmental constraints as BGW, but requires more separation energy [6]. Nonetheless, SW desalination through reverse osmosis (RO) is emerging as a technically and economically viable solution for high-return crops, such as those in greenhouses [5, 7].

RO is the most widely used membrane-based desalination technology. RO offers cost effectiveness, energy efficiency when used with energy recovery devices [8], and high salt rejection (often $> 99\%$) [9]. Consequently, Israel [10, 11], Spain [12, 13], and some US states [5], including California and Florida, are implementing, planning and/or assessing SW-RO for agriculture. RO removes all ions from SW, including monovalent ions harmful to crops (Na^+, Cl^-) and divalent ions favorable to crops ($Ca^{2+}, Mg^{2+}, SO_4^{2-}$) [14]. These nutrients must then be reintroduced to the desalinated water by addition of fertilizer.

Monovalent selective electrodialysis (MSED), a variant of conventional electrodialysis (ED), may provide an alternative to SW-RO for greenhouses. The technology possesses two main advantages. First, MSED selectively extracts damaging monovalent ions, while retaining favorable divalent ions in the desalinated water. This selective separation reduces fertilizer requirements and related expenses. Second, MSED can operate at a substantially higher recovery than RO. According to Jones et al. [15], the average recovery of SW-ED plants globally is 86% compared to SW-RO's 42%. Higher recovery saves water and reduces the volume of brine for disposal. Additional advantages of MSED

include its longer membrane lifetime, by 2-3 years [16], and greater tolerance for fouling [17] relative to RO.

The main disadvantage of MSED for SW desalination is its notably higher specific energy consumption (SEC) than that of RO [18]; RO SEC ranges from 2–4.5 kWh/m^3 [6, 19] in comparison to MSED's SEC of 3.7–15 kWh/m^3 depending on operating conditions [19, 20, 21, 22, 23]. Solar-powered desalination provides a more sustainable option than conventionally-powered desalination, because it mitigates the global warming impact of greater SEC [24]. The shift in energy prices over the past decade is rapidly altering the desalination landscape, as the electricity generated by solar energy is becoming less expensive than that generated by coal and gas power plants. The International Desalination Association has set a 2020–2025 target of using renewable energy in 20% of new desalination plants [25]. Many coastal arid regions have high solar capacity and cheap solar energy, reflecting the potential for solar-powered SW desalination.

The feasibility of SW-MSED for greenhouses depends on whether its advantages of nutrient and water savings, resulting in lower fertilizer and brine disposal costs (Appendix A), outweigh its disadvantages of greater capital and operating costs than RO. Interviews we conducted with greenhouses using RO indicate that a two-year payback period on new equipment is desired [26]. The literature has explored MSED for SW brine concentration [27, 28, 29, 30], hybrid configurations of ED with other desalination technologies for SW treatment [31, 32, 33] and MSED for BGW treatment [14, 17, 34, 35]. To our knowledge, no studies have been conducted on the characterization or application of stand-alone MSED for SW desalination for irrigation.

This study performs the first techno-economic analysis of SW-MSED for irrigation with a comparison to SW-RO, highlighting the energy cost and consumption requirements to make SW-MSED competitive with SW-RO. First, we characterize the new Fujifilm Type 16 (Fujifilm Corporation) and well-established Neosepta ACS/CMS (Astom Corporation) MSED membranes. Experiments on an average SW composition and Arabian Gulf SW composition are conducted to evaluate membrane monovalent selectivity, membrane resistance, and limiting current density. The experimentally-determined system parameters then serve as inputs to our MSED cost model. This model quantifies fertilizer savings, water savings, operating costs, and capital costs. These MSED values are compared to the capital and operating costs of RO to approximate MSED cost effectiveness: the key differences result from RO's notably lower energy consumption and membrane costs. We consider

both conventionally powered and on-grid solar-powered desalination systems in the following nations, which contain arid coastal regions with cheap and available solar power: Australia, Chile, Namibia, Spain, the United Arab Emirates, and the United States (California). Trends in desalination cost with electricity price, energy source, energy consumption, farm size, and membrane type are investigated.

2. Methods

2.1. Experimental

An MSED system contains two types of monovalent selective ion-exchange membranes, an anion exchange membrane (AEM) and cation exchange membrane (CEM). The AEMs and CEMs are placed in alternating order between two electrodes, and spacers are positioned between the membranes, as well as the membranes and electrodes, to configure the flow. AEMs and CEMs are composed of a polymer matrix embedded with positively charged groups and negatively charged groups, respectively [16]. AEMs allow monovalent anions to pass, while rejecting divalent anions and all cations. CEMs allow monovalent cations to pass, while rejecting divalent cations and all anions. An applied potential difference across the electrodes induces ion transport across the membranes; anions migrate towards the anode and cations migrate towards the cathode. Figure 1 shows this process for an MSED system with one cell pair, which includes a diluate channel, concentrate channel, CEM and AEM. MSED separates the seawater feed stream into a nutrient-rich diluate stream ($Ca^{2+}, Mg^{2+}, SO_4^{2-}$) and a concentrate stream high in monovalent ions (Na^+, Cl^-, K^+). Although MSED removes potassium, which is a nutrient for crops, it retains other divalent nutrients that would otherwise be removed by RO.

Net salt and water transport across the membrane in each compartment of the MSED stack can be written as [36]:

$$J_{s,j} = \frac{T_{s,j}^{cp} i}{zF} - L_j(C_{j,c,m} - C_{j,d,m}) \tag{1}$$

$$J_w = \frac{T_w^{cp} i}{F} + L_w(\pi_{j,c,m} - \pi_{j,d,m}) \tag{2}$$

where J is flux in $\text{mol}\cdot\text{m}^{-2}\cdot\text{s}^{-1}$, s denotes salt, w denotes water, j denotes ionic species, T is a transport number, F is Faraday's constant, L is the membrane permeability in $\text{m}\cdot\text{s}^{-1}$ for the salts and in $\text{s}\cdot\text{m}^{-1}$ for the water, C is a concentration in $\text{mol}\cdot\text{m}^{-3}$, z is the ion valence, π is osmotic pressure in bar, c denotes concentrate, d denotes diluate, and m denotes membrane. The applied

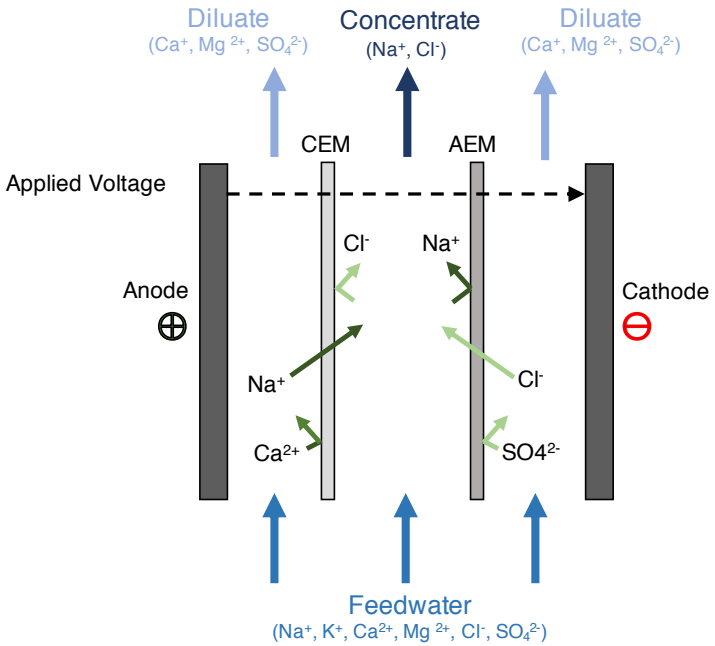

Figure 1: A simplified MSED stack containing two electrodes, CEM and AEM, with seawater as the feedwater. An applied voltage across the electrodes induces ion transport. Potassium and magnesium, not shown here, will exhibit the same behavior as sodium and calcium, respectively.

current density i is a function of the applied voltage, Donnan potentials and ohmic resistances for the membranes, diluate, and concentrate (Appendix D). The salt flux in Equation 1 depends on ion migration (first term) and ion diffusion (second term). The water flux in Equation 2 depends on electro-osmosis (first term) and water diffusion (second term).

We experimentally determine the membrane selectivity, membrane resistance, and limiting current density to characterize the MSED membranes. Details of the methods for membrane resistance and limiting current density calculations can be found in Appendix B.

2.1.1. Experimental set-up

The MSED experimental set-up contains diluate, concentrate, and electrode rinse flow circuits in a batch configuration that feed into a PCCell ED200 stack (Figure 2). The diluate and concentrate containers have a 1 L and 4 L feedwater capacity, respectively, and the electrode container has a 4 L rinse capacity. The stack is composed of 10 membrane cell pairs (total active membrane area of 0.43 m^2), 20 spacers of 0.5 mm thickness, and 2 end spacers in the electrode streams of 1 mm thickness. Two types of membrane were analyzed: Neosepta ACS/CMS membranes and Fujifilm

Table 1: Analyzed seawater ionic compositions, including an average composition and Arabian Gulf composition [37].

Concentration (g/L)	Average SW	Arabian Gulf
TDS	34.2	45.4
Na^+	10.6	14.2
Ca^{2+}	0.40	0.50
Mg^{2+}	1.26	1.77
K^+	0.38	0.46
Cl^-	19.1	24.2
SO_4^{2-}	2.65	3.55

Type 16 membranes. Table 2 includes Neosepta membrane specifications. Because the Fujifilm membranes are not yet commercially available, a specifications datasheet has not been published.

To simulate feedwater to the system, we dissolved calcium, magnesium, sodium, potassium, sulfate, and chloride in deionized water. Based on a World Health Organization data set on global variation in SW salinity [37], two compositions were considered (Table 1): a global average SW composition and Arabian Gulf SW composition because of its uniquely high salinity. An inductively coupled plasma optical emission spectrometer was used to measure diluate water composition. The electrode rinse was composed of sodium sulfate (0.2 M) to stabilize pH.

To perform experiments, we used valved-flowmeters and centrifugal pumps (Iwaki, model MD-55R (T)) to produce a steady flow of 95 LPH in the three circuits. The flow channel height is 0.5 mm. The power supply (GW-INSTEK GPR-60600) applied a voltage across the stack to drive the desalination process. A heat exchanger regulated the concentrate temperature. The stack acted as a second heat exchanger to fix the diluate temperature at 25°C.

2.1.2. Membrane permselectivity

Membrane permselectivity P quantifies a membrane's ability to selectively remove monovalent relative to divalent ions. It is defined as the ratio of divalent to monovalent transport number $T_{s,j}^{cp}$, normalized by initial ion concentration at $t = 0$:

$$P_{mon}^{div} \equiv \frac{T_{div}/w_{div,o}}{T_{mon}/w_{mon,o}} \tag{3}$$

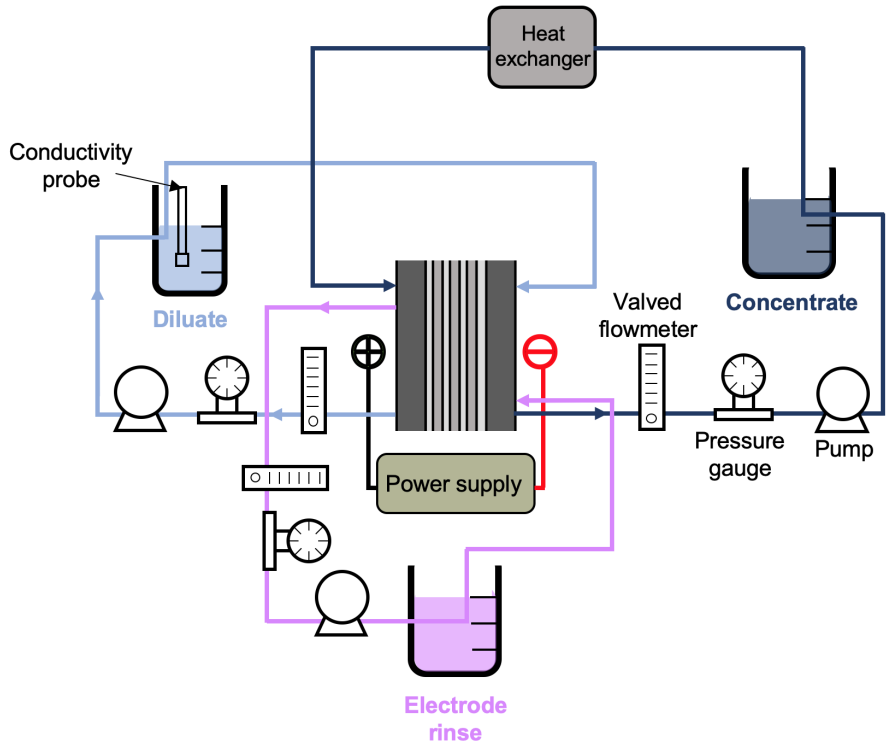

(a)

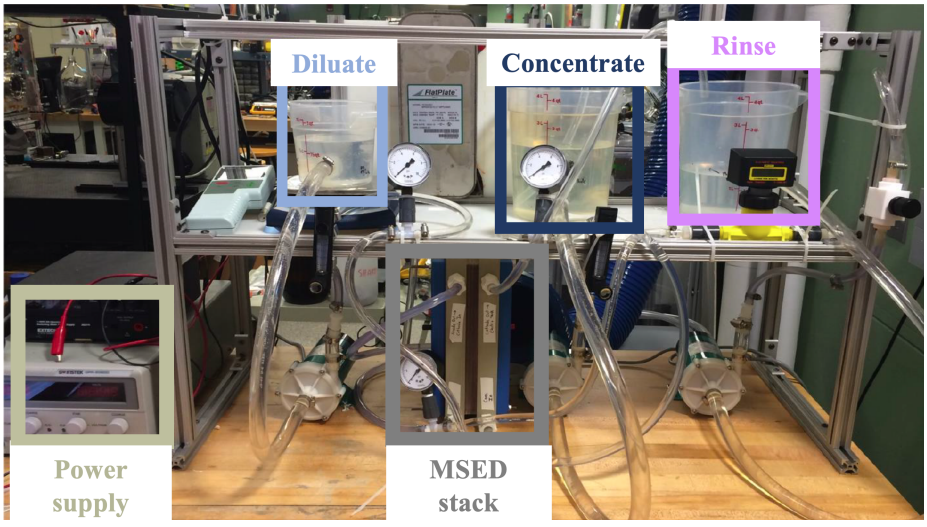

(b)

Figure 2: MSED set-up consisting of a diluate, concentrate, and rinse circuit feeding an ED200 stack (adopted from [34]).

Table 2: Detailed specification of Neosepta CMS/ACS membranes. Electrical resistance is measured on AC after equilibration with a 0.5 M NaCl solution at 25°C. [14, 38]

	CMS	ACS
Type	Strong acid (Na type)	Strong base (Cl type)
Functional group	Sulfonic acid	Ammonium
Characteristics	Monovalent cation permselectivity	Monovalent anion permselectivity
Burst strength (MPa)	≥ 0.10	≥ 0.15
Thickness (mm)	0.15	0.13
Temperature (°C)	≤ 40	≤ 40
pH	0–10	0–8

Based on Equation 1, transport number can be written as:

$$T_{s,j}^{cp} = \frac{\Delta w_j F}{i \Delta t A_m N_{cp}} \tag{4}$$

where Δw_j represents the change in ion concentration in milliequivalents relative to the initial ion concentration at $t = 0$, N_{cp} is the number of cell pairs, and A_m is the membrane area in m^2. Based on the Hittorf method, the ion diffusion term in Equation 1, which is almost three orders of magnitude less than the ion migration term [17], can be neglected. McGovern et al. [33] have validated this trend even for high salinity applications. The closer P is to zero, the greater the monovalent selectivity of the membrane. In other words, a higher permselectivity corresponds to a lower removal of monovalent ions and a less efficient MSED system.

To determine membrane selectivity, we conducted tests in which we measured the change in ion concentration in the diluate in a fixed amount of time. Simulated seawater served as feedwater in the diluate and concentrate circuits. A minimum of three tests per feedwater composition and membrane was performed to ensure repeatability. The applied current at any point in the desalination process did not exceed $0.7 i_{lim}$, a typical operating limit in commercial ED systems [39].

2.2. Cost model

Current MSED cost models in the literature [20] are tailored towards brine concentration, in which the benefit of MSED is revenue generation from salt production. For irrigation, the benefit of MSED is its fertilizer and water savings relative to RO. Consequently, we modified MSED and RO cost models to account for irrigation operating conditions and MSED savings. We considered MSED

savings as extra costs for RO systems ($\text{Cost}_{\text{extra,w}}$, $\text{Cost}_{\text{extra,f}}$). The net costs of MSED and RO after one year of operation can then be defined as:

$$\text{Cost}_{\text{total,MSED,yr}} = \text{CapEx}_{\text{MSED,yr}} + \text{OpEx}_{\text{MSED,yr}} \tag{5}$$

$$\text{Cost}_{\text{total,RO,yr}} = \text{CapEx}_{\text{RO,yr}} + \text{OpEx}_{\text{RO,yr}} + \text{Cost}_{\text{extra,w}} + \text{Cost}_{\text{extra,f}} \tag{6}$$

The CapEx indicates annual capital costs and OpEx annual operating costs of the respective systems. The following subsections describe the calculations for MSED expenses and savings. Appendix E includes details on the RO cost model.

2.2.1. MSED capital costs

MSED equipment costs are assumed to scale with membrane area. Data gathered by Sajtar and Bagley [40] and analyzed by McGovern et al. [41] yields an ED equipment cost per unit membrane area of $\text{SpCapEx}_{\text{ED}} = 750$ \$/m^2. This data accounts for plant sizes of up to 40,000 m^3/day and feed salinities of up to 7,000 mg/L. Nayar et al. [20] quote a $\text{SpCapEx}_{\text{ED}} = 600$ \$/m^2 for high salinity ED plants, including a membrane cost of \$222/m^2. Because ED and MSED systems require the same equipment, we assume equivalent equipment costs aside from the membranes ($\text{SpCapEx}_{\text{MSED,non-mem}} = 378$ \$/m^2).

Neosepta membranes cost 503 \$/m^2 at the lab scale [42] and around 180 \$/m^2 at the commercial scale [43]. Because we are interested in real-world greenhouse applications, we use the commercial price in our cost analysis. The commercial price of the Fujifilm membranes, which are still under development, is unknown. Consequently, we consider two cases for the Fujifilm membranes: 1) the commercial cost equals the lab-scale cost of 162 \$/m^2 ($A_m < 10$ m^2) [44] and 2) the commercial cost equals 58 \$/m^2, based on the lab-scale to commercial cost ratio of the Neosepta membranes (~ 2.8).

The total MSED capital cost is evaluated as:

$$\text{CapEx}_{\text{MSED}} = (\text{SpCapEx}_{\text{MSED,non-mem}} + \text{SpCapEx}_{\text{MSED,mem}}) \times A_{\text{mem}} \tag{7}$$

The required membrane area for a given desalination capacity was calculated from Nayar et al.'s MSED model [20] for a current density of 300 A/m^2 (Appendix D). The annual capital cost can be

calculated using the annuity factor (AF):

$$\mathrm{CapEx}_{\mathrm{MSED,yr}} = \frac{\mathrm{CapEx}_{\mathrm{MSED}}}{\mathrm{AF}} \tag{8}$$

$$\mathrm{AF} = \frac{1 - (\frac{1}{1+r})^T}{r} \tag{9}$$

where r corresponds to an annual interest rate of 8% [45] and T corresponds to a period of 15 years, the typical life expectancy of RO and MSED systems [46].

For PV-powered MSED, an additional term must be included in Equation 5 to account for PV capital costs. We considered capital costs for utility-scale PV ranging from 450–650 $/kWp [47, 48]. A specific yield of 1400 kWh/kWp [48, 49, 50] results in a specific capital cost of 0.32-0.46 $/kWh ($\mathrm{SpCost}_{\mathrm{PV}}$). The annual PV capital cost depends on the specific PV capital cost, the total MSED work in kWh/m^3, $\dot{W}_{\mathrm{MSED}}$, and the annual desalination capacity accounting for a 95% capacity factor [51, 52]:

$$\mathrm{CapEx}_{\mathrm{PV,MSED,yr}} = \dot{W}_{\mathrm{MSED}} \times \mathrm{SpCost}_{\mathrm{PV}} \times \dot{V}_{\mathrm{p,MSED,yr}} \tag{10}$$

The total work can be determined by modelling the MSED stack as a circuit with ohmic terms, Donnan potentials and the voltage across the electrodes (Appendix D). In this analysis, the total MSED work was equivalent to 7.0 kWh/m^3. The energy requirements may be optimized depending on various parameters, such as current density, membrane resistance, spacer thickness and recovery ratio. However, the purpose of this study is to provide a comparison of MSED to RO for typical operating conditions. This energy value for SW desalination is consistent with the literature and industry for recoveries of up to 86% and current densities ranging from 300 to 600 A/m^2 [53, 54].

2.2.2. MSED operating costs

The total OpEx includes energy, membrane replacement, maintenance, labor and chemical costs:

$$\begin{aligned}\mathrm{OpEx}_{\mathrm{MSED,yr}} = \mathrm{OpEx}_{\mathrm{energy,MSED,yr}} + \mathrm{OpEx}_{\mathrm{mem,MSED,yr}} + \mathrm{OpEx}_{\mathrm{maint,MSED,yr}} \\ + \mathrm{OpEx}_{\mathrm{labor,MSED,yr}} + \mathrm{OpEx}_{\mathrm{chem,MSED,yr}}\end{aligned} \tag{11}$$

Annual energy expenses are a function of the total MSED work, the cost of electricity $\mathrm{Cost}_{\mathrm{electricity}}$,

and the annual system capacity:

$$\mathrm{OpEx}_{\mathrm{energy,MSED,yr}} = \dot{W}_{\mathrm{MSED}} \times \mathrm{Cost}_{\mathrm{electricity}} \times \dot{V}_{\mathrm{p,MSED,yr}} \tag{12}$$

The cost of electricity varies with location and energy source. We considered greenhouses located in the Middle East, South America, North America, Africa, and Australia and powered by conventional (i.e., fossil fuels) and solar energy sources.

We selected an MSED membrane lifetime of 7 years, based on the typical 5–10 year range [17]. Consequently, the membranes must be replaced twice during the project duration at the 7-year and 14-year mark:

$$\mathrm{OpEx}_{\mathrm{mem,MSED,yr}} = \frac{\mathrm{CapEx}_{\mathrm{mem,MSED}}}{\mathrm{AF}} \left(\frac{1}{(1+r)^7} + \frac{1}{(1+r)^{14}} \right) \tag{13}$$

The labor cost of one full-time employee was assumed to be $\$50,000$/yr [40]. The specific annual costs of chemicals and maintenance were assumed to be 2.1 \$/m^2-yr and 8.5 \$/m^2-yr [20, 40, 41], respectively. The remaining annual operating expenses can then be written as:

$$\begin{aligned} &\mathrm{OpEx}_{\mathrm{labor,MSED,yr}} + \mathrm{OpEx}_{\mathrm{chem,MSED,yr}} + \mathrm{OpEx}_{\mathrm{maint,MSED,yr}} \\ &\qquad = 50000 + 2.1\mathrm{A}_{\mathrm{mem,tot}} + 8.5\mathrm{A}_{\mathrm{mem,tot}} \end{aligned} \tag{14}$$

2.2.3. MSED water savings

The extra water cost incurred by RO because of its lower water recovery than MSED is defined as:

$$\mathrm{Cost}_{\mathrm{extra,w}} = \left(\frac{1}{\mathrm{RR}_{\mathrm{RO}}} - \frac{1}{\mathrm{RR}_{\mathrm{MSED}}} \right) \times \left(\mathrm{Cost}_{\mathrm{feed}} + \mathrm{Cost}_{\mathrm{brine}} \right) \times \dot{V}_{\mathrm{p,yr}} \tag{15}$$

SW-RO recoveries typically range from 40% to 50% [6]. We assumed an RO recovery of 42%, the average for SW-RO plants around the world [15]. Less data exists on SW-ED recoveries, because the technology is less commonly used for this application. We considered an MSED recovery of 86%, the average recovery for SW-ED plants globally [15], as well as a lower recovery of 66% [55, 56]. The cost of feedwater supply corresponds to the energy cost of seawater intake pumping. In this analysis, a fixed intake energy requirement of 0.02 kWh/m^3 based on the literature [57] results in

Table 3: Fertilizer cost Cost_f to add one ppm of divalent ions to one m^2 of a greenhouse.

Ion	Cost_f ($\$\cdot\text{m}^{-2}\cdot\text{ppm}^{-1}$)
Ca^{2+}	2.69 x 10^{-3}
Mg^{2+}	1.71 x 10^{-3}

the following minimal cost of feedwater:

$$\text{Cost}_\text{feed} = 0.02 \times \text{Cost}_\text{electricity} \tag{16}$$

SW desalination brine is usually disposed via surface water discharge [15, 54] (Appendix A). The cost of surface water discharge ranges from 0.03 $\$/\text{m}^3$ to 0.30 $\$/\text{m}^3$ [9, 54, 58, 59]. The desalination capacity for a given farm size is based on the assumption that one hectare of farm requires a desalination capacity of 60 m^3/day/ha [17, 34].

2.2.4. MSED fertilizer savings

Fertilizer contains essential macronutrients for crop growth: nitrate, phosphate, potassium, calcium, magnesium, and sulfate. Various salts are dissolved in water to attain the desired nutrient levels, including: gypsum, epsom, potassium chloride and/or sulfate, ammonium nitrate and/or sodium nitrate, and ammonium phosphate. Epsom and gypsum introduce magnesium and calcium, respectively. Sulfate is added to fertilizer with multiple salts (e.g., gypsum, epsom, potassium sulfate). Consequently, only calcium and magnesium were considered in MSED fertilizer savings, representing a lower bound on possible nutrient savings.

Epsom and gypsum are cost-effective and sustain pH levels without altering the concentration of other nutrients. The addition of 4.09×10^{-4} kg of epsom to 1 m^2 of soil yields a 50 ppm increase in magnesium [60]. The addition of 3.06×10^{-4} kg of gypsum to 1 m^2 of soil yields a 110 ppm increase in calcium [61]. Table 3 shows the costs of adding magnesium and calcium to soil in greenhouses based on current gypsum and epsom prices [62, 63]. Experimentally-determined, average CEM permselectivities were used to characterize the nutrient retention of the Neosepta and Fujifilm membranes. Although the target composition of irrigation water is crop-specific, our aim is to calculate a first-order approximation of MSED fertilizer savings independent of crop. Based on general water quality recommendations in Table 4, we set the final concentration of calcium, the

Table 4: Water quality recommendations for agriculture [11, 46, 64].

Ion	Concentration (ppm)
Ca^{2+}	80-200
Mg^{2+}	30-80
Na^{+}	Low as possible
SO_4^{2-}	> 50
Cl^{-}	> 20

Table 5: Typical RO ion percent reductions for BGW: $100\ \frac{C_{div,o}-C_{div,f|\mathrm{RO}}}{C_{div,i}}$ [14].

Ion	Ion reduction (%)
Ca^{2+}	90
Mg^{2+}	99
Na^{+}	97
SO_4^{2-}	99
Cl^{-}	98

dominant ion in fertilizer cost savings, equal to 200 mg/L[1]. The final sodium concentration is near or equal to zero. RO final concentrations, which serve as the baseline of comparison to MSED, were determined from the feedwater composition and ion percent reductions in Table 5. Assuming one growing season per year, the extra fertilizer cost of RO ($\mathrm{Cost_{extra,f}}$) can then be evaluated as:

$$\mathrm{Cost_{extra,f}} = [(C_{div,o} - C_{div,f|\mathrm{RO}}) - (C_{div,o} - C_{div,f|\mathrm{MSED}})] \times \mathrm{Cost_f} \times \mathrm{A_{farm}} \tag{17}$$

where C_{div} refers to divalent ion concentration in mg/L, o refers to initial, f refers to final, and $\mathrm{A_{farm}}$ is the greenhouse area in ha.

3. MSED membrane characterization

This section provides experimental results of membrane monovalent selectivity for a bench-scale MSED system containing Fujifilm Type 16 and Neosepta ACS/CMS membranes. Results for mem-

[1]This value yields an upper limit of MSED fertilizer savings in order to provide a first approximation of how MSED's optimal performance compares to RO's performance. In reality, MSED fertilizer savings will be lower as a result of feedwater composition and membrane property limitations. Figure F.22 demonstrates how fertilizer savings vary with final calcium concentration.

brane resistance and limiting current density can be found in Appendix B. We analyze an average seawater composition and Arabian Gulf composition, which contains a higher salinity than that of typical seawater. Trends in ion concentration with desalination process time and membrane selectivity with total dissolved solids (TDS) and membrane type are investigated. The results demonstrate the monovalent selectivity of the MSED membranes and consequently the fertilizer savings offered by MSED relative to RO for greenhouses.

3.1. Transient ion concentration

For both seawater compositions and MSED membranes, normalized cation and anion concentrations vary linearly with desalination process time in a given experiment (Figure 3). This trend is consistent with the literature [65, 66]. Monovalent ion concentration decreases at a faster rate than divalent ion concentration, reflecting the monovalent selective nature of the Fujifilm and Neosepta membranes.

In order to travel across the membranes, ions must party or completely shed their hydration shell. Therefore, a lower hydration energy corresponds to a greater ion removal over time. The cation concentration-time slopes increase with decreasing hydration energy: magnesium (1904 kJ/mol), calcium (1592 kJ/mol), sodium (405 kJ/mol), potassium (321 kJ/mol) [67, 68]. Similarly, the anion concentration-time slopes increase with decreasing hydration energy: sulfate (1145 kJ/mol) and chloride (369 kJ/mol) [68].

3.2. Membrane permselectivity

The Fujifilm and Neosepta membranes demonstrate notable selectivity towards monovalent ions for average and Arabian Gulf SW compositions (Table 6). For the treatment of average SW, the Fujifilm calcium permselectivity of 0.22 ± 0.09 corresponds to a factor of 3.2-7.7 reduction of sodium relative to calcium and magnesium permselectivity of 0.19 ± 0.05 to a factor of 4.2-7.1 reduction of sodium relative to magnesium. The Fujifilm sulfate permselectivity of 0.17 ± 0.04 corresponds to a factor of 4.8-7.7 reduction of chloride relative to sulfate. In comparison, the Neosepta calcium permselectivity of 0.33 ± 0.06 corresponds to a factor of 2.6-3.7 reduction of sodium relative to calcium and magnesium permselectivity of 0.21 ± 0.07 to a factor of 3.6-7.1 reduction of sodium relative to magnesium. The Neosepta sulfate permselectivity of 0.17 ± 0.04 corresponds to a factor of 3.3-6.3 reduction of chloride relative to sulfate.

For the treatment of Arabian Gulf SW, the Fujifilm calcium permselectivity of 0.54 ± 0.06 corresponds to a factor of 1.7-2.1 reduction of sodium relative to calcium and magnesium permselectivity of

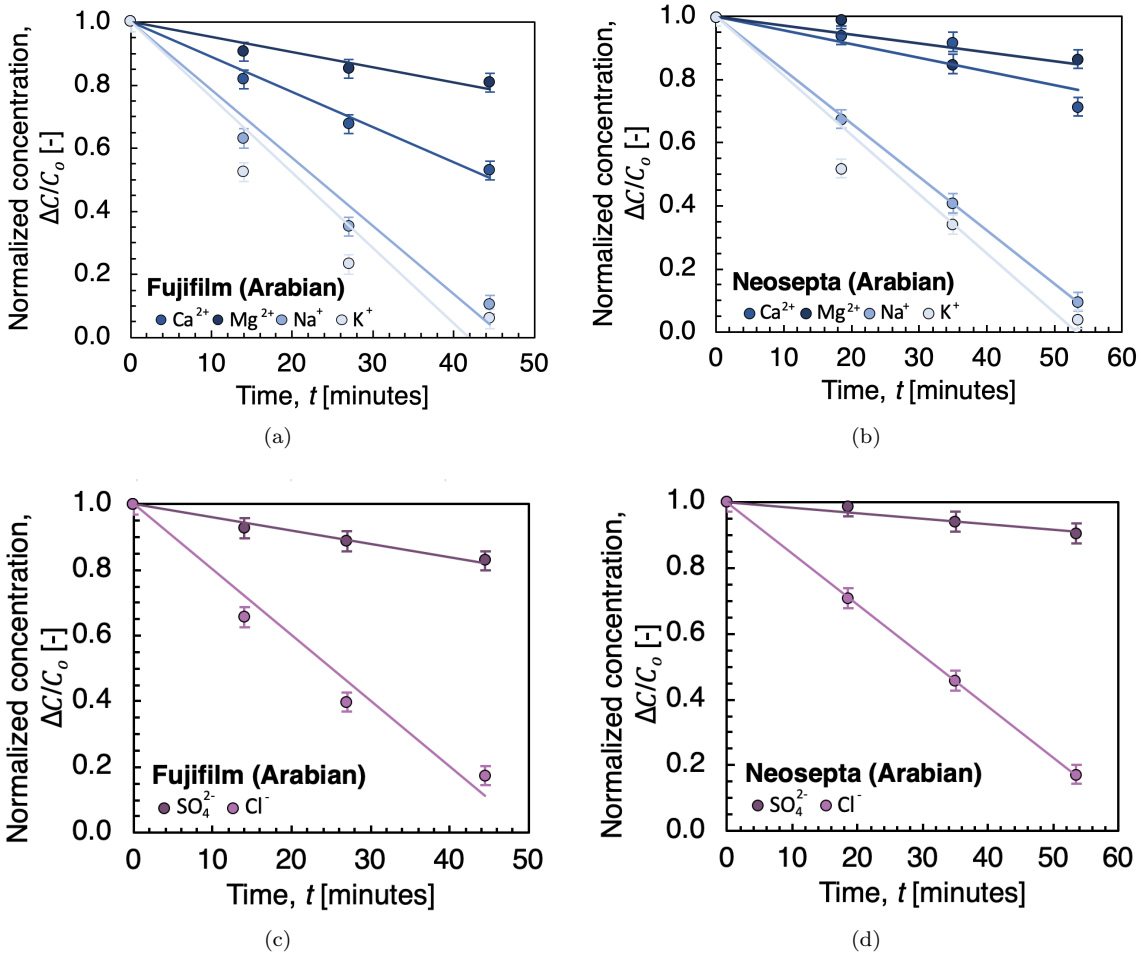

Figure 3: Normalized cation ($Ca^{2+}, Mg^{2+}, Na^+, K^+$) and anion ($SO_4^{2-}, Cl^-$) concentrations of Neosepta and Fujifilm membranes as a function of desalination process time for two seawater compositions.

Table 6: Permselectivity values of Fujifilm and Neosepta membranes for average seawater and Arabian Gulf compositions. We include permselectivities relative to potassium for completeness. Because potassium is also a nutrient for crops, its divalent selectivity values do not contribute to possible MSED fertilizer savings.

Composition	Membrane	$P_{Na^+}^{Ca^{2+}}$	$P_{Na^+}^{Mg^{2+}}$	$P_{K^+}^{Ca^{2+}}$	$P_{K^+}^{Mg^{2+}}$	$P_{Cl^-}^{SO4^{2-}}$
Average	Fujifilm	0.22 ± 0.09	0.19 ± 0.05	0.20 ± 0.08	0.16 ± 0.04	0.17 ± 0.04
	Neosepta	0.33 ± 0.06	0.21 ± 0.07	0.28 ± 0.06	0.18 ± 0.06	0.23 ± 0.07
Arabian Gulf	Fujifilm	0.54 ± 0.06	0.29 ± 0.08	0.44 ± 0.03	0.23 ± 0.06	0.26 ± 0.08
	Neosepta	0.31 ± 0.07	0.19 ± 0.07	0.25 ± 0.07	0.13 ± 0.02	0.12 ± 0.08

0.29 ± 0.08 to a factor of 2.7-4.8 reduction of sodium relative to magnesium. The Fujifilm sulfate permselectivity of 0.17 ± 0.04 corresponds to a factor of 2.9-5.6 reduction of chloride relative to sulfate. In comparison, the Neosepta calcium permselectivity of 0.31 ± 0.07 corresponds to a factor of 2.6-4.2 reduction of sodium relative to calcium and magnesium permselectivity of 0.19 ± 0.07 to a factor of 3.9-8.3 reduction of sodium relative to magnesium. The Neosepta sulfate permselectivity of 0.17 ± 0.04 corresponds to a factor of 5-25 reduction of chloride relative to sulfate.

The Fujifilm membranes outperform the Neosepta membranes for the average seawater composition (TDS = 34.2 g/L), while a substantial decrease in Fujifilm membrane performance occurs at the higher salinity of the Arabian Gulf (TDS = 45.4 g/L). In contrast, the Neosepta membranes experience a moderate improvement in performance for the Arabian Gulf relative to seawater composition. Figure 4 demonstrates trends in permselectivity over a wider TDS range of 1.4–45.4 g/L. The Fujifilm membranes show lower cation permselectivity, i.e., greater monovalent selectivity, and comparable anion permselectivity for TDS < 35 g/L relative to the Neosepta CEMs. The differences in membrane performance with salinity may result from their respective target feedwater salinities: Fujifilm membranes are tailored towards lower salinity, brackish water applications. Neosepta membranes have been designed for high salinity applications to concentrate seawater or seawater brine for salt production. Other factors that impact membrane selectivity, including co-ion concentration and membrane duration, are discussed in Appendix C.

4. MSED and RO total costs

This section investigates whether MSED can serve as an alternative to RO in coastal greenhouses under typical operating conditions. Solar-powered desalination was also studied to mitigate the environmental impact of SW-MSED's greater energy consumption compared to SW-RO. Our cost analysis focuses on six nations experiencing high water scarcity (Figure 5), high photovoltaic (PV)

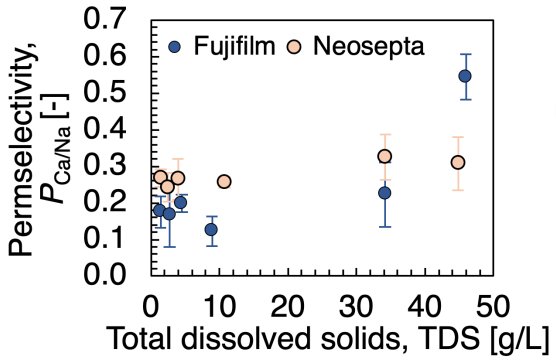

(a)

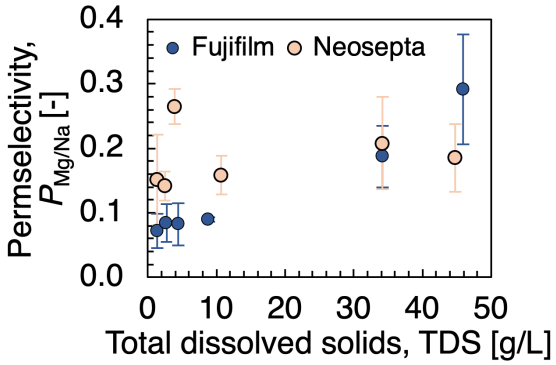

(b)

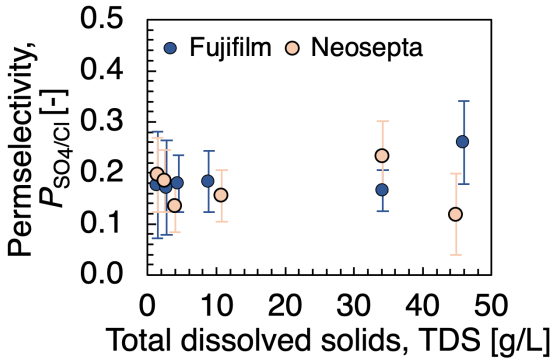

(c)

Figure 4: Neosepta and Fujifilm permselectivity as a function of TDS for waters containing 1.4 g/L to 45.4 g/L. The brackish water experimental data is from previous studies we conducted [17, 34].

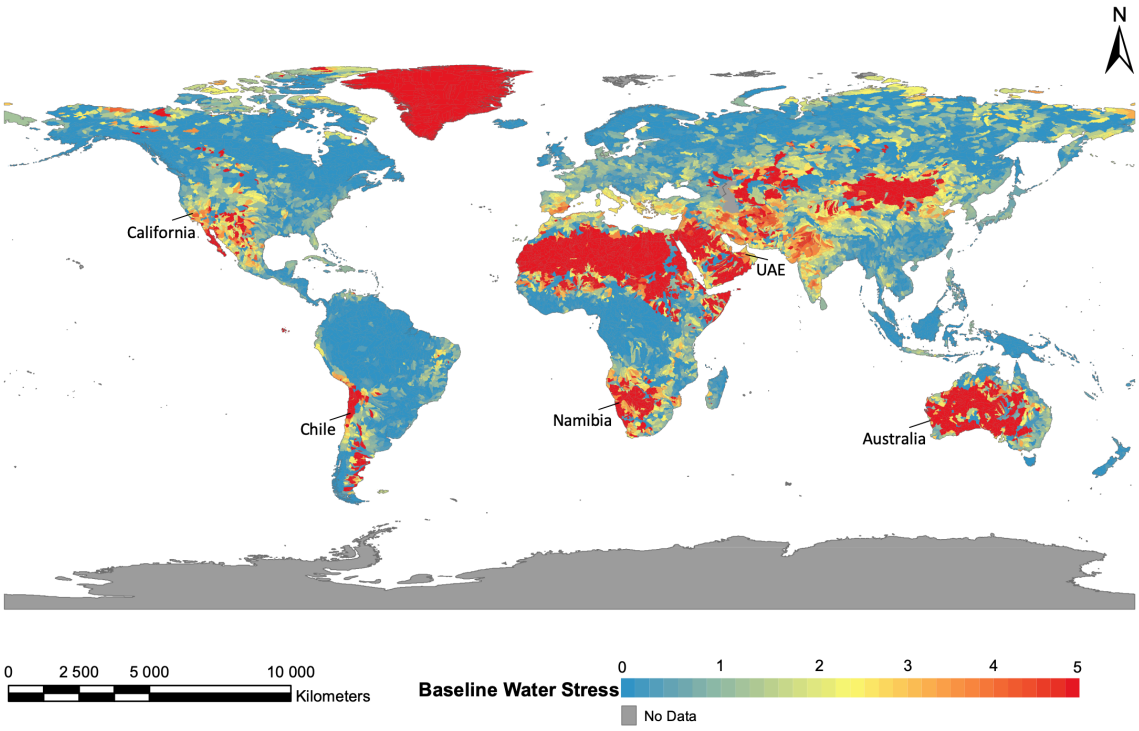

Figure 5: Current global baseline water stress (data from World Resources Institute's Aqueduct project [69]). Baseline water stress represents the ratio of total withdrawals to total renewable supply in a given area. A higher value indicates more competition among users for water. Areas considered in this study are labelled.

specific yield (Figure 6), and low PV levelized cost of energy (LCOE) (Table 7) in coastal areas: Australia, the United States (California), Chile, Namibia, Spain, and the United Arab Emirates. These countries, with the exception of Namibia, are also global leaders in the desalination space.

MSED savings relative to RO were determined based on experimental results in Section 3. We considered these savings as extra costs incurred by RO to calculate an adjusted RO system cost for the six countries. For a 7 kWh/m^3 SEC for MSED and 3.5 kWh/m^3 SEC for RO, RO and MSED costs were compared for three different MSED membrane prices: 1) 58 \$/m^2 (Fujifilm projected commercial price), 2) 162 \$/m^2 (Fujifilm lab-scale price), and 3) 180 \$/m^2 (Neosepta commercial price). This comparison enabled us to identify cases in which the technologies are competitive, as well as the cost requirements for cases in which the technologies are not competitive (i.e., MSED exceeds RO cost).

4.1. MSED savings

Based on our experimental results, the total average Fujifilm and Neosepta savings for average SW are 9,334 \$/ha-yr and 9,291 \$/ha-yr, respectively (Table 8). The sensitivity of MSED savings to

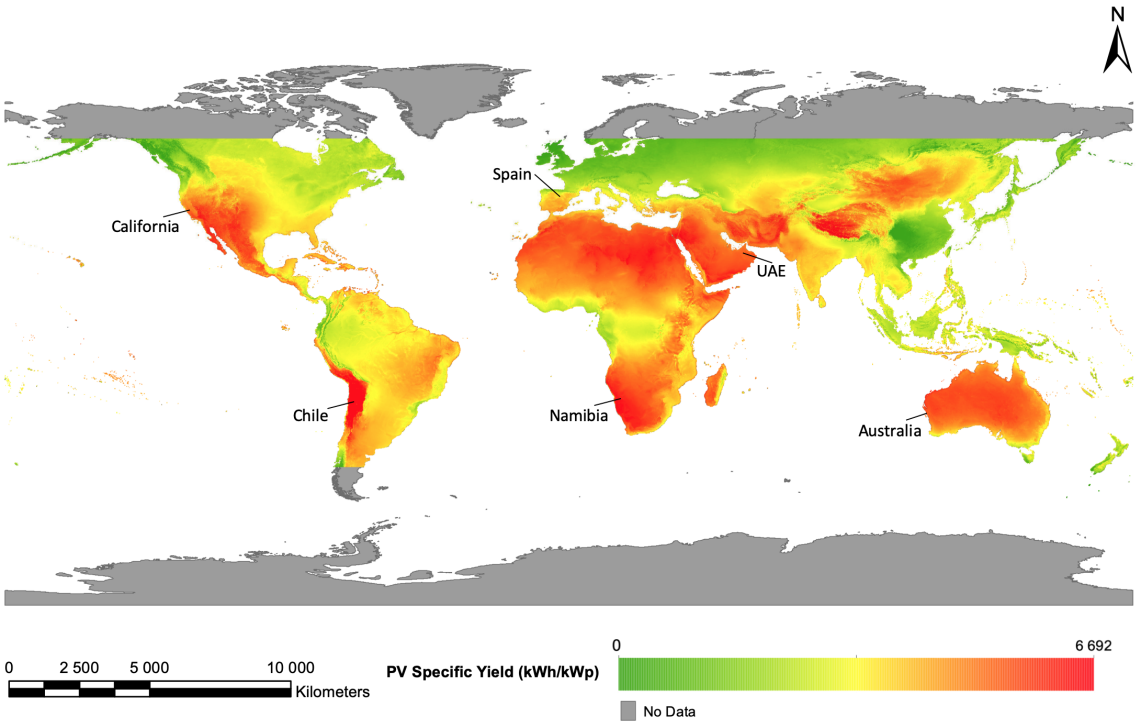

Figure 6: Global PV specific yield (data from ESMAP's Global Solar Atlas [70]). Areas considered in this study are labelled.

Table 7: LCOE of conventional and PV energy sources in Australia [71, 72, 73], U.S. [74, 75], Chile [72, 73, 76], Namibia [72, 77], Spain [72, 76] and the UAE [72, 78, 79], including recent solar project costs.

	Conventional ($/MWh)	PV ($/MWh)
Australia	227	32 – 82 (recent: 27–36)
California (U.S.)	71	52 – 65
Chile	160	33 – 60 (recent: 27–36)
Namibia	114	78 – 140
Spain	123	39 – 59
U.A.E.	76 – 111	35 – 57 (recent: 17)

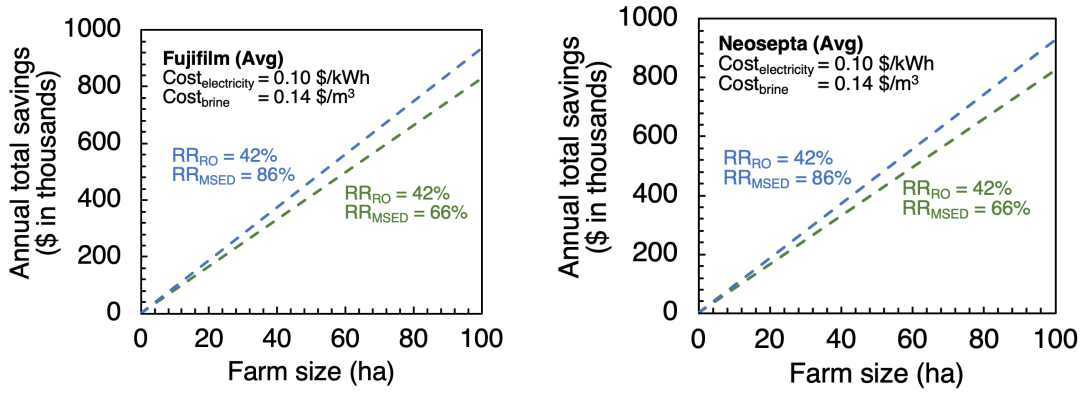

(a) (b)

Figure 7: Annual total MSED savings of the Fujifilm and Neosepta membranes as a function of recovery ratio and farm size for fixed electricity and brine disposal costs.

various parameters is shown in Table 9. Fertilizer savings are relatively insensitive to membrane type and feedwater salinity in the SW range: the values for the Arabian Gulf are within 4% of those for average SW (Table F.16). Water savings are very sensitive to system recovery and brine disposal costs (Figure F.21(a)) and relatively insensitive to cost of electricity (Figure F.21(b)). Both water and fertilizer savings scale linearly with farm size (Figures F.21(c,d)). Consequently, the total MSED savings exhibit a linear relationship with farm size (Figure 7).

Table 8: Average fertilizer and water savings ($/ha-yr) offered by MSED Fujifilm and Neosepta membranes relative to RO for average SW composition. Water savings are based on a brine disposal cost of 0.14 $/m^3, electricity cost of 0.10 $/m^3, MSED recovery of 86% and RO recovery of 42%.

	$\text{Cost}_{\text{RO,extra,f}}$	$\text{Cost}_{\text{RO,extra,w}}$	$\text{Cost}_{\text{RO,extra,tot}}$
Neosepta	5,692	3,599	9,291
Fujifilm	5,735	3,599	9,334

4.2. Conventionally powered desalination

Figure 8 demonstrates the average specific desalination costs of Fujifilm MSED for conventional energy sources in the six surveyed nations. These specific costs are independent of farm size, i.e.,

Table 9: The impact of system recovery, membrane selectivity, membrane type, SW salinity, brine disposal costs, electricity costs and farm size on total savings offered by MSED relative to RO. This analysis is conducted by holding all parameters except the variable of consideration fixed.

	RR_{MSED}	$P^{\text{div}}_{\text{mon}}$	$\text{Cost}_{\text{brine}}$	$\text{Cost}_{\text{electricity}}$	A_{farm}	membrane	SW salinity
$\text{Cost}_{\text{RO,extra,tot}}$	↑	↑	↑	—	↑	—	—

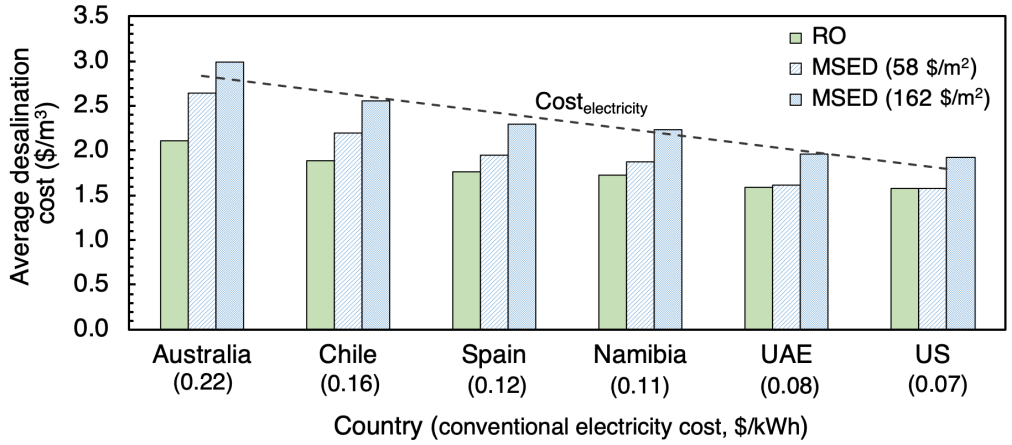

Figure 8: Average desalination specific cost as a function of technology and country (i.e., electricity cost) for conventional energy sources.

system capacity. RO cost includes the extra fertilizer and water costs relative to MSED. Conventional MSED with a 162 $/m^2 membrane cost ranges from 1.96–2.99 $/m^3 and with a 58 $/m^2 membrane cost from 1.57–2.64 $/m^3, in comparison to RO's 1.58–2.11 $/m^3. MSED fertilizer and water savings substantially reduce the disparity between the two technologies for SW desalination. For a membrane cost of 162 $/m^2, MSED costs an average of 72% more than RO without savings and 30% more than RO with savings. For a membrane cost of 58 $/m^2, MSED costs an average of 46% more than RO without savings and 10% more than RO with savings.

The difference in electricity cost accounts for the variable cost ratio of MSED to RO across the six nations (Figure 9). A lower electricity cost results in lower specific operating costs, while specific MSED savings remain constant. In the US and UAE, which have the lowest electricity costs, MSED is within 1% of RO for 58 $/m^2 and 22% of RO for 162 $/m^2. In comparison, the greatest disparity between MSED and RO occurs in Australia, which has the highest electricity cost: MSED is 25% and 42% greater than RO for membrane costs of 58 $/m^2 and 162 $/m^2, respectively. Consequently, potential for MSED adoption in California and the UAE may exist once the less expensive Fujifilm membranes are commercially available; in Namibia and Spain, where MSED costs are within 10% of RO, growers may be willing to overlook this moderate price difference if brine management is a central issue. With current membrane costs ranging from 162-180 $/m^2, MSED savings do not fully offset its greater capital and operating costs relative to RO regardless of electricity cost. Figure 10 and Table 10 include the breakdown of RO and MSED costs for these representative systems. On average, MSED capital expenses must be reduced by 57% or operating expenses by 39% for MSED

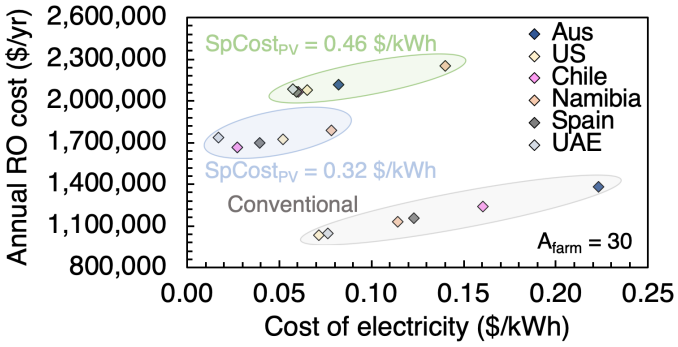

(a)

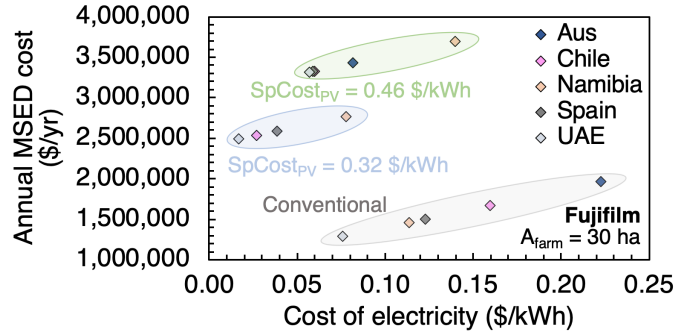

(b)

Figure 9: (a) RO and (b) Fujifilm MSED total annual costs as a function of electricity cost and energy source for a fixed farm size of 30 ha.

to be competitive with RO.

These expenses may be mitigated by lowering MSED energy requirements (Figure 11(a)) and membrane price (Figure 11(b)). A 62% decrease in energy consumption (2.66 kWh/m^3) makes MSED on par with RO for a membrane cost of 162 \$/m^2 and average electricity cost of 0.13 \$/kWh. A recent SW-ED project in Singapore shows potential for decreasing the typically demanding ED energy consumption [80]: the 3800 m^3/day (63 ha farm) demonstration plant has achieved an energy consumption of 2.4 kWh/m^3. Membrane acquisition comprises 30% (Fujifilm) to 32% (Neosepta) of total MSED capital expenses, while membrane replacement comprises 19% (Fujifilm) to 21% (Neosepta) of total MSED operating expenses. A membrane cost of \$3/m^2 results in equivalent MSED and RO costs for an average electricity cost of 0.13 \$/kWh and MSED SEC of 7 kWh/m^3. As electricity cost decreases, permissible SEC and membrane price for competitive MSED increase (Table 11). In other words, less cost improvements to MSED are necessary in nations with lower electricity cost.

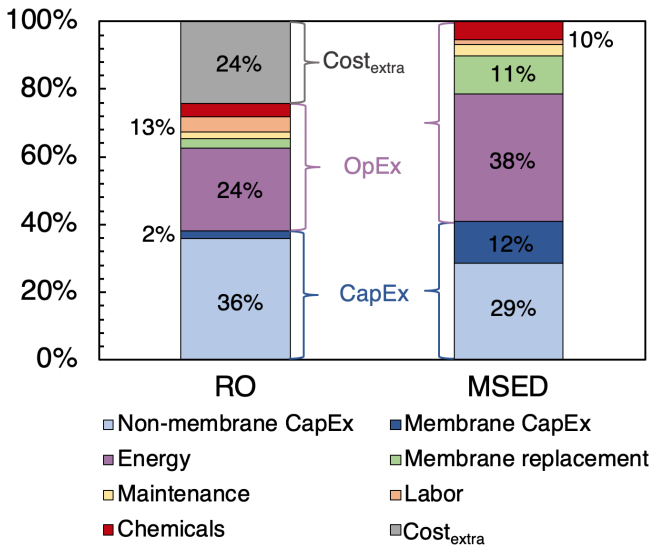

Figure 10: Cost breakdown of conventional MSED and RO including extra fertilizer and water costs of RO relative to MSED for a membrane cost of 162 \$/m^2 and average electricity cost of 0.13 \$/kWh.

Table 10: Annual costs (\$ in thousands) of RO and MSED systems with variable membrane cost for a 30 ha farm in Spain and typical SECs of 3.5 and 7 kWh/m^3, respectively. We selected this country because of its advanced agriculture sector, which is beginning to implement SW-RO [3], and its representative electricity cost of 0.12 \$/kWh for conventional sources.

	RO	Fujifilm (58 \$/m^2)	Fujifilm (162 \$/m^2)	Neosepta (180 \$/m^2)
Membrane	27	66	185	205
Non-membrane	415	431	431	431
Total CapEx	442	497	616	636
Energy	283	566	566	566
Membrane replacement	33	61	170	189
Labor	53	50	50	50
Chemicals	46	20	20	20
Maintenance	20	83	83	83
Total OpEx	435	780	889	908
Extra fertilizer cost	172	–	–	–
Extra water cost	108	–	–	–
Extra costs	280	–	–	–
Annual expenses	1,157	1,277	1,505	1,544

Table 11: Variations in MSED membrane price (given in \$/m^2) and SEC with electricity cost.

Cost$_{electricity}$ (\$/kWh)	SEC (kWh/m^3)		
	58 \$/m^2	100 \$/m^2	162 \$/m^2
< 0.08	7.0	5.0	2.7
0.11–0.12	5.5	4.4	2.7
0.22	4.6	4.0	2.7

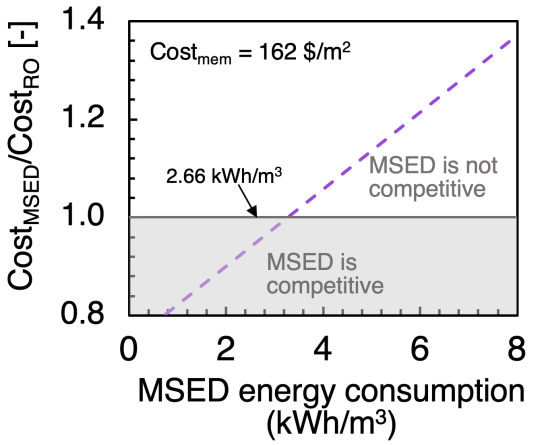

(a)

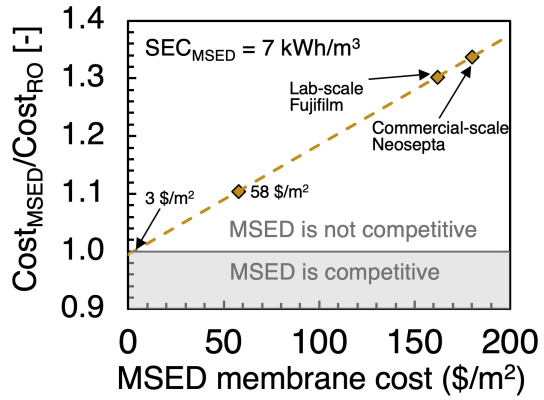

(b)

Figure 11: The ratio of MSED to RO system costs for (a) variable specific energy consumption (SEC) at fixed membrane cost and (b) variable membrane cost at fixed SEC for an average electricity cost of 0.13 $/kWh across the six selected nations. We assume that MSED is competitive with RO when their costs are equal, i.e., the ratio is equal to one. In reality, MSED might be competitive with RO at a higher ratio depending on the importance of brine management in a given location.

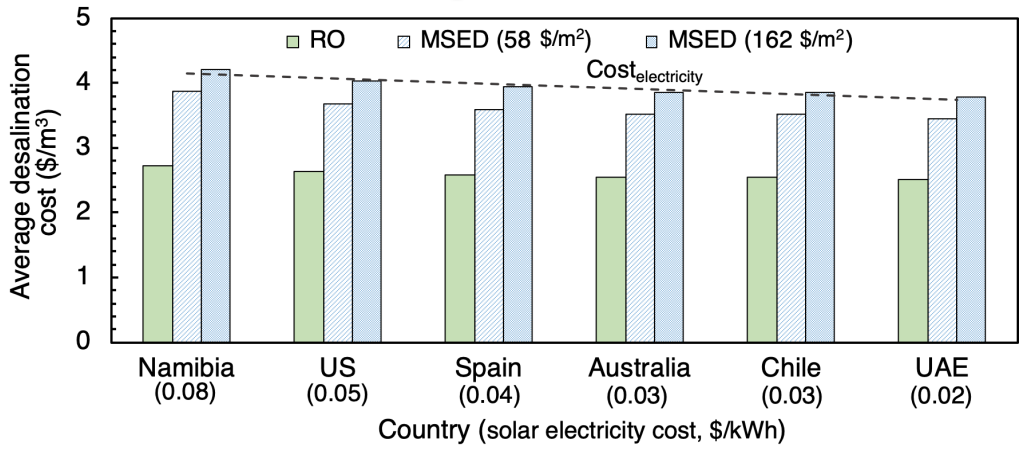

Figure 12: Average desalination specific cost as a function of technology and country (i.e., electricity cost) for solar energy sources.

4.3. Solar-powered desalination

Figure 12 displays the average specific desalination costs for conventional energy sources and the six selected countries. Solar-powered desalination costs are significantly higher than that of conventionally powered desalination even for cases in which PV electricity and capital costs are set to a minimum in each country. For these minimum cases, PV-MSED ranges from 3.79–4.22 \$/m^3 for a 162 \$/m^2 MSED membrane price and 3.44–3.87 \$/m^3 for a 58 \$/m^2 MSED membrane price, compared to PV-RO from 2.51–2.72 \$/m^3. The disadvantage of higher PV capital expenses greatly outweighs the benefit of lower solar electricity costs in the surveyed countries, as shown in Figure 13 and Table 12. Because PV capital costs were assumed to depend linearly on energy consumption, the disparity between MSED and RO is much larger than that for conventional energy. PV-MSED costs 39% and 53% more than PV-RO for MSED membrane costs of 58 \$/m^2 and 162 \$/m^2, respectively.

Given current desalination SECs, PV capital costs must be decreased from 0.32–0.46 \$/kWh to 0.10–0.20 \$/kWh, depending on the country, in order to make solar-powered desalination on par with conventionally powered desalination. More cost-effective or energy-dense PV cells and lower desalination SEC may also alleviate greater solar-powered desalination costs. For example, a membrane cost of 162 \$/m^2 and 62% reduction in MSED energy consumption (2.66 kWh/m^3) requires a PV capital expense of approximately 0.20 \$/kWh for the six considered countries.

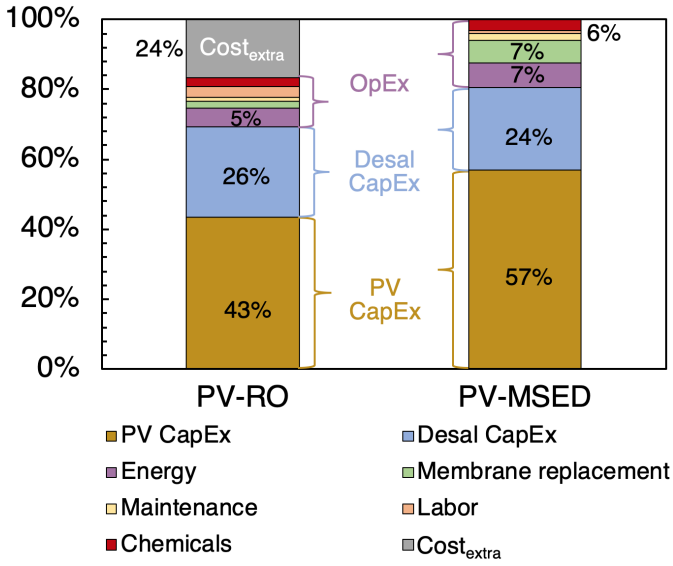

Figure 13: Cost breakdown of solar-powered MSED and RO including the extra fertilizer and water costs of RO relative to MSED.

Table 12: Annual costs ($ in thousands) of PV-RO and PV-MSED systems with variable membrane cost for a 30 ha farm in Spain and typical SECs of 3.5 and and 7 kWh/m^3, respectively. A PV capital cost of 0.32 $/kWh and electricity cost of 0.04 $/kWh are used in the case study. The annual energy cost is significantly lower for solar ($90K for RO and $179K for MSED) compared to conventionally powered desalination ($283K for RO and $566K for MSED). However, the additional PV capital costs ($736k for RO and $1,472K for MSED) result in solar-powered desalination as the less economical option.

	RO	Fujifilm (58 $/m^2)	Fujifilm (162 $/m^2)	Neosepta (180 $/m^2)
Desalination	442	497	616	636
PV	736	1,472	1,472	1,472
Total CapEx	1,178	1,969	2,088	2,108
Energy	90	179	179	179
Membrane replacement	33	61	170	189
Labor	53	50	50	50
Chemicals	46	20	20	20
Maintenance	20	83	83	83
Total OpEx	242	393	502	521
Extra fertilizer cost	172	–	–	–
Extra water cost	108	–	–	–
Extra costs	280	–	–	–
Annual expenses	1,700	2,362	2,590	2,629

4.4. Cost trends in greenhouse size

In reality, the specific desalination cost decreases with farm size or system capacity[2] (Figure 14), unlike the average values we have considered thus far. Because specific MSED savings are constant, larger farms should benefit more from implementing MSED. However, the moderate curvature in specific cost ($/m^3) with typical greenhouse area appears to diminish when annual costs ($/yr) are considered, i.e., when the specific cost is multiplied by system capacity or farm size. Consequently, linear trends in annual capital and operating expenses with farm size are observed in Figure 15. In other words, the average specific desalination costs used in this analysis are representative: a 50 ha farm will incur approximately twice the desalination cost of a 25 ha farm, assuming specific energy requirements and electricity costs are the same.

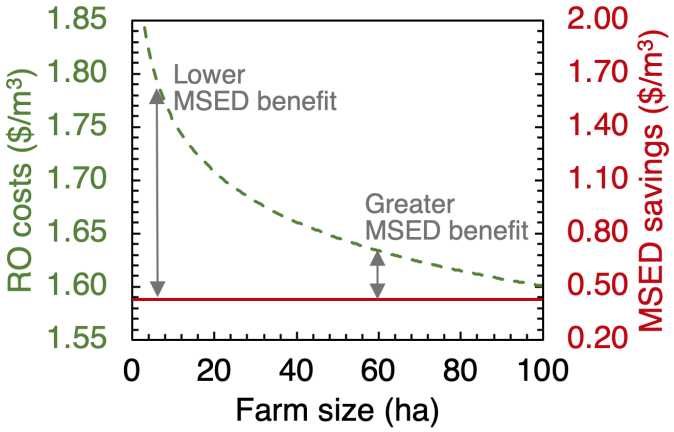

Figure 14: RO specific cost independent of MSED (i.e., not including extra fertilizer and water costs) and MSED specific savings as a function of farm size or desalination capacity for a coastal greenhouse located in Australia. MSED specific savings are constant, because savings linearly vary with farm size.

5. Conclusions

This study conducts the first techno-economic analysis of seawater monovalent selective electrodialysis for irrigation with a comparison to seawater reverse osmosis. We analyze energy, fertilizer and water consumption, as well as electricity price, requirements at which either technology will be more cost competitive. Neosepta ACS/CMS and Fujifilm Type 16 monovalent selective electrodialysis membranes were tested on two seawater compositions to characterize membrane selectivity and sav-

[2]The larger the farm size, the greater the required desalination capacity (m^3/day). As desalination capacity increases, specific capital expenses ($/m^3) decrease. Consequently, specific desalination cost ($/m^3) is lower for larger desalination systems and farms.

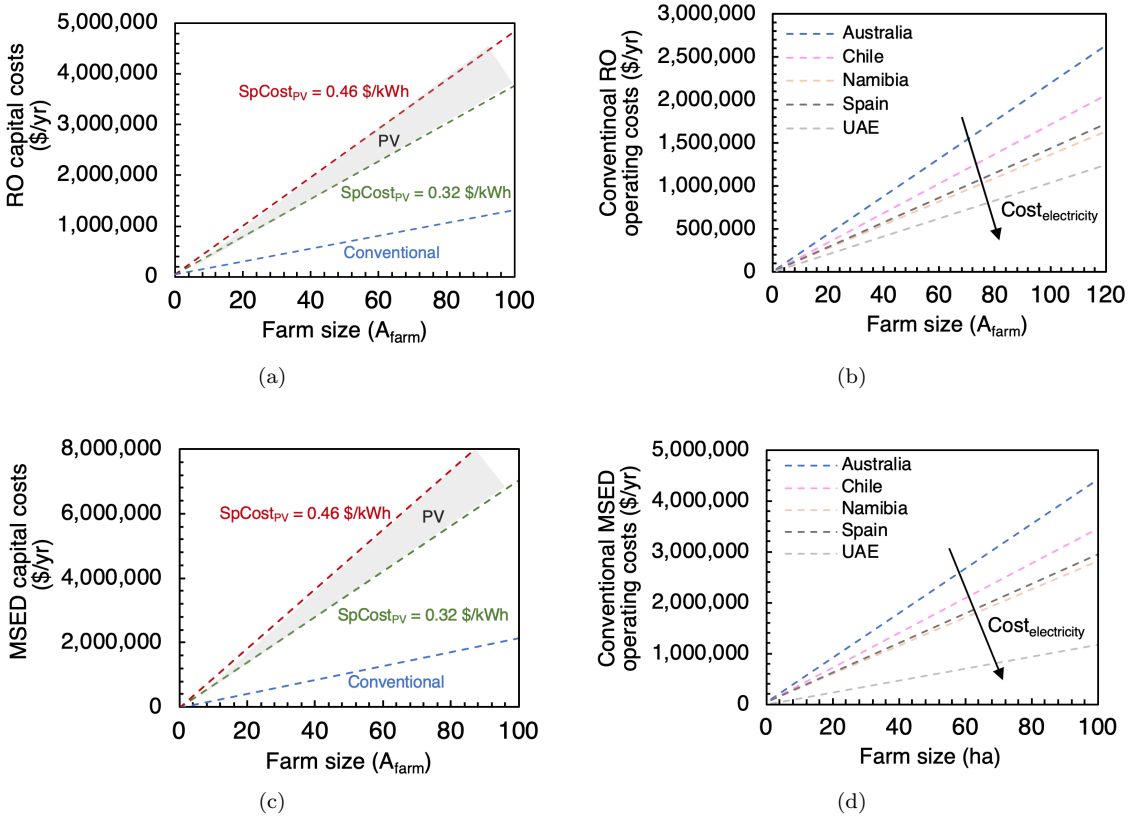

Figure 15: (a, c) RO and MSED capital costs as a function of energy source, including the minimum PV case of 0.32 $/kWh and maximum PV case of 0.46 $/kWh, and farm size. (b, d) Conventionally powered RO and MSED operating costs as a function of electricity cost and farm size.

ings offered by monovalent selective electrodialysis relative to reverse osmosis. These monovalent selective electrodialysis savings were compared to its greater capital and operating costs to determine adoption potential in coastal greenhouses for six countries with different electricity prices. Tables 13 and 14 contain cost summaries of conventionally powered and solar-powered monovalent selective electrodialysis and reverse osmosis systems. The following detailed conclusions have been reached:

1. Monovalent selective electrodialysis membranes demonstrate notable selectivity towards monovalent ions for average and Arabian Gulf seawater compositions. For the treatment of average seawater, the Fujifilm cation exchange membranes remove 3.2-7.7 sodium per calcium ion and 4.2-7.1 sodium per magnesium ion. The Neosepta cation exchange membranes remove 2.6-3.7 sodium per calcium ion and 3.6-7.1 sodium per magnesium ion. For the treatment of Arabian Gulf seawater, the Fujifilm CEMs remove 1.7-2.1 sodium per calcium ion and 2.7-4.8 sodium per magnesium ion. The Neosepta cation exchange membranes remove 2.6-4.2 sodium per

calcium ion and 3.9-8.3 sodium per magnesium ion. The Fujifilm membranes outperform the Neosepta membranes for feedwaters containing a TDS $\leq$ 35 g/L.

2. Based on monovalent selective electrodialysis experimental results, monovalent selective electrodialysis annual savings of 9,334 \$/ha-yr for Fujifilm and 9,292 \$/ha-yr for Neosepta are determined for the average seawater composition. The Arabian Gulf seawater savings are within 4% of these representative values. These savings are considered in our cost model as extra reverse osmosis costs. They significantly reduce the disparity between monovalent selective electrodialysis and reverse osmosis for seawater desalination, although the extent depends on monovalent selective electrodialysis membrane cost, electricity cost, and energy requirements. For example, a lower electricity cost results in a lower total system cost, while the specific monovalent selective electrodialysis savings remain fixed. Consequently, countries with lower electricity cost (e.g., US, UAE) will benefit more from monovalent selective electrodialysis savings than those with higher electricity cost (e.g., Australia, Chile).
3. Current monovalent selective electrodialysis membranes range in cost from Fujifilm's 162 \$/m^2 at the lab-scale to Neosepta's 180 \$/m^2 at the commercial scale. Given these costs, monovalent selective electrodialysis savings do not offset the technology's greater capital and operating costs relative to reverse osmosis. Monovalent selective electrodialysis costs an average of 72% more than reverse osmosis without savings and 30% more than reverse osmosis with savings. For the six considered countries, an monovalent selective electrodialysis energy consumption of 2.7 kWh/m^3, compared to the characteristic 7 kWh/m^3, results in equivalent monovalent selective electrodialysis and reverse osmosis costs.
4. If we assume that the Fujifilm membranes still in the R&D phase will show the same cost trend with scale as the widely-used Neosepta membranes, Fujifilm membranes may eventually cost 58 \$/m^2 for greenhouse applications. At this price point, monovalent selective electrodialysis is far more competitive with reverse osmosis: monovalent selective electrodialysis costs an average of 10% more than reverse osmosis across the six countries. In the US and UAE ($\text{Cost}_{\text{electricity}} < 0.08$ \$/kWh), monovalent selective electrodialysis cost is within 1% of reverse osmosis. Consequently, monovalent selective electrodialysis adoption may be favorable once the less expensive Fujifilm membranes are commercially available. If monovalent selective electrodialysis energy consumption can be lessened, this membrane price point is competitive with reverse osmosis in Spain and Namibia for a 5.5 kWh/m^3 ($\text{Cost}_{\text{electricity}} = 0.11 - 0.12$ \$/kWh) and Australia for a 4.6 kWh/m^3 ($\text{Cost}_{\text{electricity}} = 0.22$ \$/kWh).

Table 13: Comparison of reverse osmosis and monovalent selective electrodialysis specific costs ($/m^3) for two monovalent selective electrodialysis membrane prices ($/m^2) and conventional electricity prices ranging from 0.07–0.22 $/kWh. Results include the cost difference between monovalent selective electrodialysis and reverse osmosis and requirements for monovalent selective electrodialysis to compete with reverse osmosis.

	Cost ($/m^3)	$\text{Cost}_{\text{MSED}-\text{RO}}/\text{Cost}_{\text{RO}}$ (%)	Reqs. for competitive MSED
RO	1.58–2.11	–	–
MSED (180 $/m^2)	1.96–2.99	24–42	Average of 57% CapEx reduction (e.g., membranes) or 39% OpEx reduction (e.g., SEC)
MSED (58 $/m^2)	1.57–2.64	−0.63–25	$\text{Cost}_{\text{electricity}} < 0.11$ $/kWh: Fujifilm membrane commercialization. $\text{Cost}_{\text{electricity}} = 0.11$–$0.22$ $/kWh: SEC reduction of 21%-37%.

Table 14: Comparison of PV-RO and PV-monovalent selective electrodialysis specific costs ($/m^3) for two membrane costs ($/m^2) and solar electricity prices ranging from 0.02–0.08 $/kWh. Results include the cost difference between PV-MSED and PV-RO, as well as the difference between PV and conventionally (conv) powered desalination. Given current desalination SECs, PV capital costs must be decreased from 0.32-0.46 $/kWh to 0.10-0.20 $/kWh, depending on electricity price, in order for solar-powered desalination's cost to be on par with with conventionally powered desalination.

	Cost ($/m^3)	$\text{Cost}_{\text{MSED}-\text{RO}}/\text{Cost}_{\text{RO}}$ (%)	$\text{Cost}_{\text{PV}-\text{conv}}/\text{Cost}_{\text{conv}}$ (%)
PV-RO	2.51–2.72	–	29–59
PV-MSED (180 $/m^2)	3.79–4.22	51–55	41–93
PV-MSED (58 $/m^2)	3.44–3.87	37–42	47-119

5. For solar-powered desalination to be economical, PV capital costs of 0.32-0.46 $/kWh need to be greatly reduced. Given current desalination energy consumption, a capital cost of 0.10-0.20 $/kWh, depending on the country, makes solar-powered desalination on par with conventionally powered desalination.

6. Acknowledgments

Y.D. Ahdab would like to thank the National Science Foundation and the Martin Foundation for funding the research reported in this paper. Additional support was provided by the Centers for Mechanical Engineering Research and Education at MIT and SUSTech (MechERE Centers at MIT and SUSTech).

Appendix A. Brine disposal costs

Table A.15 includes information on brine disposal and treatment methods, including the treatment principle and the cost. Current methods for disposing of desalination brine are surface water discharge, sewer discharge, deep-well injection, evaporation ponds and land application. A method is selected depending on a variety of factors, including: brine composition and quantity; geographic location; availability of receiving site (e.g., surface body); and capital and operating costs. Over 90% of seawater desalination plants use surface water discharge back into the ocean, while sewer discharge, deep-injection wells and land application are almost exclusively used by brackish water desalination plants [59].

Table A.15: Brine disposal and treatment principles and cost ($/m^3 of rejected brine) [9, 54, 58]. A desirable alternative to liquid brine disposal is fully dewatering the brine to a solid product, so as to achieve Zero Liquid Discharge (ZLD).

Method	Principle	Cost ($/m^3)
Surface water discharge	Discharged into surface water	0.03–0.30
Sewer discharge	Discharged into existing sewage collection system	0.30–0.66
Deep-well injection	Injected into porous subsurface rock formations	0.33–2.65
Evaporation ponds	Evaporated, resulting in salt accumulation at pond bottom	1.18–10.04
Land application	Irrigates salt-tolerant crops and grasses	0.74–1.95
ZLD	Concentrated and evaporated to yield freshwater and solid	0.66–26.41

Appendix B. Limiting current density and membrane resistance

The membrane resistance and limiting current density of the Fujifilm Type 16 membranes and Neosepta ACS/CMS membrane were experimentally determined for various dilutions of NaCl solutions containing a TDS ranging from 0.8–35 g/L [17, 34]. These NaCl results serve as a lower bound on the membrane resistance and limiting current density for any multi-ionic solution[3], providing a benchmark for SW behavior.

[3]The lower current density of NaCl compared to multi-ionic solutions is a result of the applied current being carried by other cations in addition to sodium, the dominant cation in SW. Due to the monovalent selectivity of the CEMs, the membranes preferentially transport sodium compared to divalent cations across the membrane. Consequently, the limiting current is not only a function of sodium concentration in multi-ionic solutions.

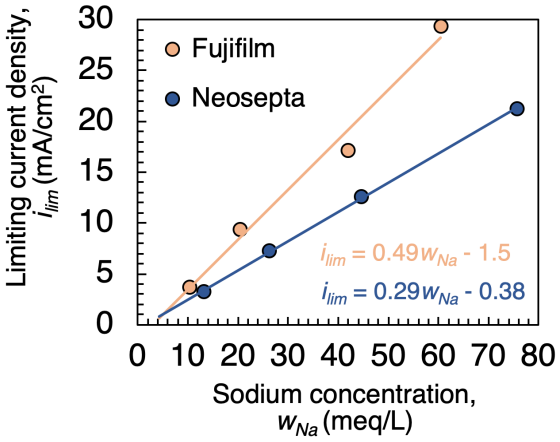

Figure B.16: Limiting current density of Neosepta and Fujifilm membranes for various dilutions of NaCl solution.

Appendix B.1. Methods

Current-voltage experiments at constant diluate and concentrate conductivity ($K_d = K_c = K$) were run to determine the membrane resistance and limiting current density. These tests were conducted for NaCl solutions containing a TDS of 800, 1500, 3000, 5000, 10,000, 22,000 and 35,000 mg/L. The CEM and AEM resistances are assumed equal. At each conductivity, the membrane resistance is evaluated based on the slope of a linear fit of V_{stack} versus the applied current from Equations D.1 and D.2:

$$m = (2N_{cp} + 1)\bar{r}_m + \frac{2N_{cp}h}{\sigma K} + \frac{2h_r}{\sigma K_r} \tag{B.1}$$

The limiting current density is calculated using the Cowan and Brown method [81]. For each conductivity, the stack electrical resistance ($\Delta V_{stack}/I$) is plotted as a function of the inverse of applied current ($1/I$). The inverse of the limiting current ($1/I_{lim}$) occurs at the minimum point at which the electrical resistance begins to increase.

Appendix B.2. Limiting current density

Operating an MSED system at or above the limiting current can greatly impede MSED membrane performance by worsening monovalent selectivity [17, 34]. Consequently, the limiting current is a crucial parameter in MSED system optimization. Figure B.16 demonstrates the linear dependence of limiting current on sodium concentration for the Fujifilm and Neosepta membranes. The Fujifilm membranes possess the advantage of a higher limiting current density at a given sodium concentration, i.e., they can tolerate a higher operating current without jeopardizing performance.

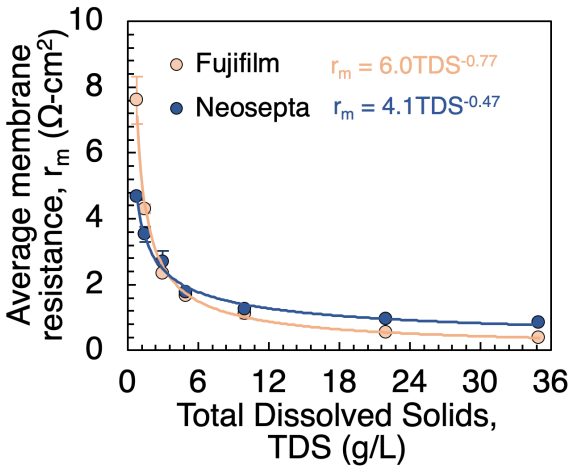

Figure B.17: CEM and AEM resistance of Neosepta and Fujifilm membranes for various dilutions of NaCl solution.

Appendix B.3. Membrane resistance

Figure B.17 demonstrates the power dependence of membrane resistance on water TDS, matching trends in the literature [65, 66]. In the region of interest for SW desalination, the Fujifilm membranes appear to possess the advantage of lower resistive losses relative to the Neosepta membranes. Although Arabian Gulf SW TDS exceeds this range, the membrane resistance remains relatively flat in the seawater salinity range and can be extrapolated for any salinity based on the resistance curves.

Appendix C. Additional factors impacting membrane permselectivity

Aside from salinity, other factors that may impact MSED membrane selectivity are ionic composition and membrane age. In previous studies, we showed that ionic composition influences selectivity for BGWs, which varies greatly in composition with location [17, 34]. Unlike BGW, SW has relatively constant ionic composition even if different salinities. Consequently, ionic composition is likely not a key determinant in MSED membrane performance for SW compositions. Figure C.18 illustrates the performance of two sets of Neosepta membranes: new (i.e., first use) and used (i.e., over 2 years of use). The results suggest that membrane performance may decrease with use within the 5–10 year lifetime of MSED membranes.

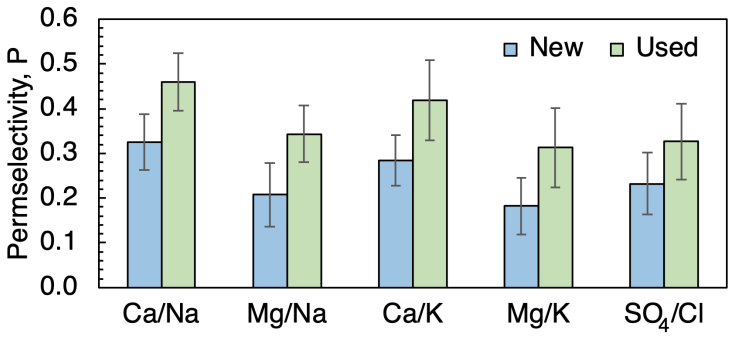

Figure C.18: The permselectivity of average SW for new Neosepta ACS/CMS membranes (i.e., first use) and used Neosepta ACS/CMS membranes (i.e., over 2 years of use).

Appendix D. MSED stack as a circuit

The MSED stack power can be calculated by modelling an MSED cell pair as a circuit with ohmic terms $\bar{r}$ and Donnan potentials E_{AEM} and E_{CEM}:

$$V_{cp} = i_k \left(2\bar{r}_{m,k} + \frac{\bar{r}_{m,k}}{N_{cp}} + \frac{\bar{r}_{d,k}}{\sigma} + \frac{\bar{r}_{c,k}}{\sigma} + \frac{2\bar{r}_{r,k}}{N_{cp}} \right) + E_{AEM} + E_{CEM} \tag{D.1}$$

where N_{cp} is number of cell pairs and r denotes the rinse solution. The spacer shadow effect σ of 0.72 $\pm$0.09 [17] and membrane resistances $\bar{r}_m$ (Appendix C) were experimentally determined. The circuit resistances are the ratio of flow channel height h to electrical conductivity K of a given stream (e.g., $\bar{r}_{d,k} = h/K_{d,k}$). The voltage across the MSED stack is the sum of the voltage across each cell pair and the voltage across the electrodes V_{el}:

$$V_{\text{stack,MSED}} = N_{cp} V_{cp} + V_{el} \tag{D.2}$$

The stack power can then be defined as:

$$\dot{W}_{\text{stack,MSED}} = \Sigma_{k=1}^{N} V_{\text{stack,MSED}} \text{ x } i_k \text{ x } A_{mem} \tag{D.3}$$

Appendix E. RO cost model

Appendix E.1. RO capital costs

We used the capital cost estimator tool on Desaldata [82] to determine the CapEx. Desaldata contains a comprehensive database of the specific capital cost $\text{SpCapEx}_{\text{RO,day}}$ ($\$/\text{m}^3 - \text{day}$) of real-

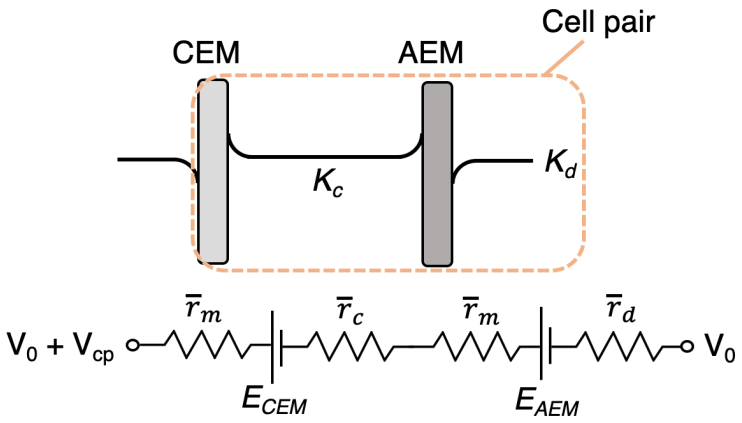

Figure D.19: Circuit diagram of MSED system.

world seawater RO desalination plants. DesalData's cost estimator considers plant size, feedwater salinity, pretreatment type, and various other factors and is based on an RO energy consumption of 3.5 kWh/m^3, half that of the MSED system. Our input parameters were the average and Arabian Gulf feedwater salinities from Table 1, standard pretreatment, typical intake/outfall and permitting, and desalination capacities that vary with farm size. Based on the assumption that 1 hectare of farm requires a desalination capacity of 60 m^3/day [17, 34], the specific capital costs for 5–100 ha greenhouses range from 1856–2455 \$/m^3 − day. The total CapEx required for an RO desalination project can then be calculated as:

$$\mathrm{CapEx_{RO}} = \mathrm{SpCapEx_{RO,day}} \times \dot{V}_{\mathrm{p,RO,day}} \tag{E.1}$$

where $\mathrm{V_{p,RO,day}}$ is volume flow rate of product water produced per day based on a capacity factor (CF) of 95%. The annual CapEx is determined using the annuity factor:

$$\mathrm{CapEx_{RO,yr}} = \frac{\mathrm{CapEx_{RO}}}{\mathrm{AF}} \tag{E.2}$$

For PV-powered RO, an additional term must be included in Equation E.2 to account for PV capital costs. The PV capital cost depends on the total RO work in kWh/m^3, $\dot{W}_{\mathrm{RO}}$, the specific PV capital cost, and annual system capacity:

$$\mathrm{CapEx_{PV,RO,yr}} = \dot{W}_{\mathrm{RO}} \times \mathrm{SpCost_{PV}} \times \dot{V}_{\mathrm{p,RO,yr}} \tag{E.3}$$

Appendix E.2. RO operating costs

The total OpEx includes energy costs, membrane replacement costs, labor costs and maintenance costs:

$$\mathrm{OpEx}_{\mathrm{RO,yr}} = \mathrm{OpEx}_{\mathrm{energy,RO,yr}} + \mathrm{OpEx}_{\mathrm{mem,RO,yr}} + \mathrm{OpEx}_{\mathrm{maint,RO,yr}} + \mathrm{OpEx}_{\mathrm{labor,RO,yr}} + \mathrm{OpEx}_{\mathrm{chem,RO,yr}} \quad \text{(E.4)}$$

Annual energy expenses are a function of the total RO work, cost of electricity, and annual system capacity:

$$\mathrm{OpEx}_{\mathrm{energy,RO,yr}} = \dot{W}_{\mathrm{RO}} \times \mathrm{Cost}_{\mathrm{electricity}} \times \dot{V}_{\mathrm{p,RO,yr}} \quad \text{(E.5)}$$

According to DesalData [82], membrane capital cost is approximately 6.5% of the total system CapEx. We selected a membrane lifetime of 5 years, based on the 3–7 year range in the literature [83]. Consequently, the membranes must be replaced twice during the project duration at the 5-year and 10-year mark:

$$\mathrm{OpEx}_{\mathrm{mem,RO,yr}} = \frac{0.065 \times \mathrm{CapEx}_{\mathrm{RO}}}{\mathrm{AF}} \left(\frac{1}{(1+r)^5} + \frac{1}{(1+r)^{10}} \right) \quad \text{(E.6)}$$

DesalData [82] also reports relatively constant SW-RO operating costs for chemicals (0.07 \$/m^3), maintenance work (0.03 \$/m^3), and labor (0.08 \$/m^3):

$$\mathrm{OpEx}_{\mathrm{maint,RO,yr}} + \mathrm{OpEx}_{\mathrm{labor,RO,yr}} + \mathrm{OpEx}_{\mathrm{chem,RO,yr}} = 0.18 \times \dot{V}_{\mathrm{p,RO,yr}} \quad \text{(E.7)}$$

Appendix F. Additional trends in RO and MSED costs

This section includes trends in MSED savings with brine disposal cost, cost of electricity, farm size, as well as in MSED and RO costs with feedwater salinity, farm size, energy source, and electricity cost, for a final calcium concentration of 200 mg/L. Figure F.22 demonstrates how MSED fertilizer savings vary with final calcium concentration.

Table F.16: Average fertilizer savings in $/ha of MSED Fujifilm and Neosepta membranes for average SW and Arabian Gulf SW compositions.

	Average SW	Arabian Gulf
Neosepta	5,692	5,517
Fujifilm	5,735	5,443

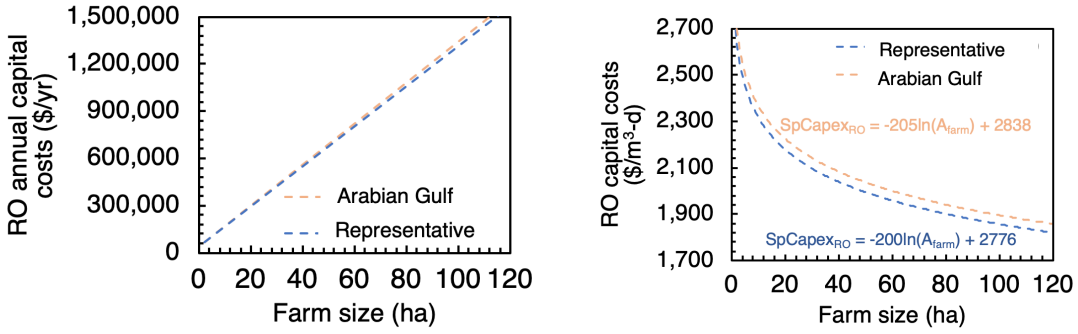

(a) (b)

Figure F.20: (a) Specific and (b) annual capital costs of RO as a function of SW feed salinity and farm size. The difference between average SW (35 g/L) and the Arabian Gulf (45 g/L) is minimal at scale. The same trend is expected for MSED capital costs.

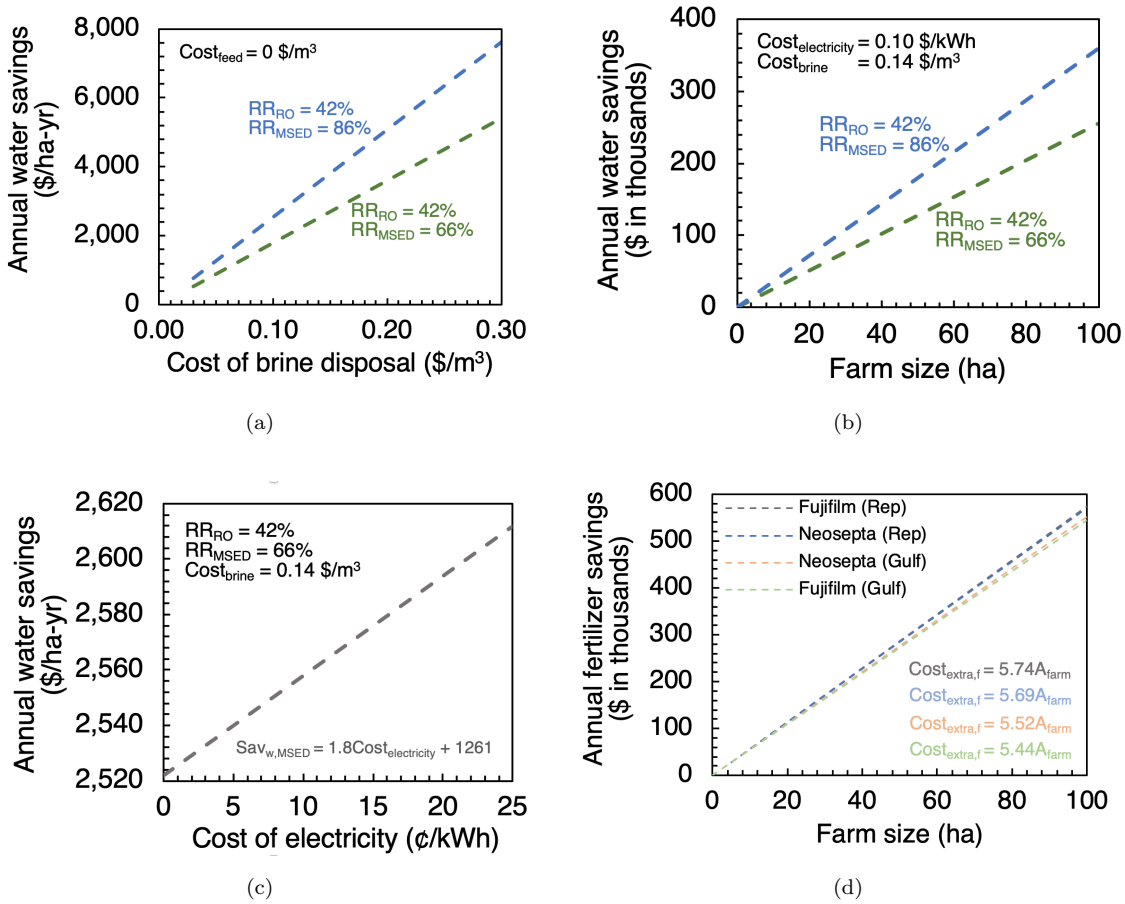

Figure F.21: Annual water and fertilizer savings of MSED as a function of brine disposal cost, electricity cost and farm size

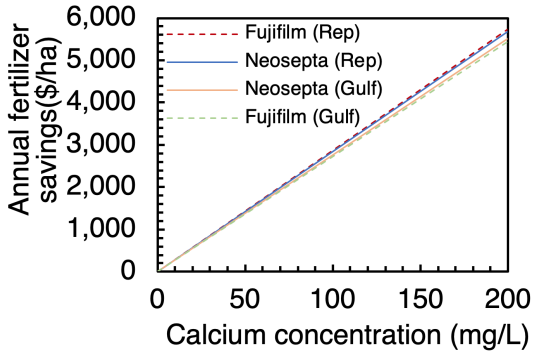

Figure F.22: Annual fertilizer savings offered by MSED as a function of final calcium concentration. In this study, we consider the upper limit of Ca = 200 mg/L. In reality, fertilizer savings may be lower depending on feedwater composition and membrane properties.

References

[1] United Nations, World water development report 2020: Water and climate change, accessed June 10, 2020 (March 2020).
URL https://unesdoc.unesco.org/ark:/48223/pf0000372985.locale=en

[2] J. Foley, A five-step plan to feed the world, accessed May 15, 2020.
URL https://www.nationalgeographic.com/foodfeatures/feeding-9-billion/

[3] J. Maestre-Valero, D. Martínez-Granados, V. Martínez-Alvarez, J. Calatrava, Socio-economic impact of evaporation losses from reservoirs under past, current and future water availability scenarios in the semi-arid segura basin, Water Resources Management 27 (5) (2013) 1411–1426. doi:10.1007/s11269-012-0245-4.

[4] A. Ben-Gal, U. Yermiyahu, S. Cohen, Fertilization and blending alternatives for irrigation with desalinated water, Journal of Environmental Quality 38 (2) (2009) 529–536. doi:10.2134/jeq2008.0199.

[5] V. Martínez-Alvarez, B. Martin-Gorriz, M. Soto-García, Seawater desalination for crop irrigation—a review of current experiences and revealed key issues, Desalination 381 (2016) 58–70. doi:https://doi.org/10.1016/j.desal.2015.11.032.

[6] J. Kim, K. Park, D. R. Yang, S. Hong, A comprehensive review of energy consumption of seawater reverse osmosis desalination plants, Applied Energy 254 (2019) 113652. doi:https://doi.org/10.1016/j.apenergy.2019.113652.

[7] J. M. Beltrán, S. Koo-Oshima, Water desalination for agricultural applications, Tech. rep., Rome, Italy (2006).
URL http://www.fao.org/3/a-a0494e.pdf

[8] C.-S. Karavas, K. G. Arvanitis, G. Papadakis, Optimal technical and economic configuration of photovoltaic powered reverse osmosis desalination systems operating in autonomous mode, Desalination 466 (2019) 97–106.
URL https://doi.org/10.1016/j.desal.2019.05.007

[9] L. F. Greenlee, D. F. Lawler, B. D. Freeman, B. Marrot, P. Moulin, Reverse osmosis desalination: Water sources, technology, and today's challenges, Water Research 43 (9) (2009)

2317–2348. doi:https://doi.org/10.1016/j.watres.2009.03.010.
URL http://www.sciencedirect.com/science/article/pii/S0043135409001547

[10] N. Avni, M. Eben-Chaime, G. Oron, Optimizing desalinated sea water blending with other sources to meet magnesium requirements for potable and irrigation waters, Water Research 47 (7) (2013) 2164–2176. doi:10.1016/j.watres.2013.01.018.

[11] U. Yermiyahu, A. Tal, A. Ben-Gal, A. Bar-Tal, J. Tarchitzky, O. Lahav, Rethinking desalinated water quality and agriculture, Science 318 (5852) (2007) 920–921. doi:10.1126/science.1146339.

[12] C. Garcia, F. Molina, D. Zarzo, 7 year operation of a BWRO plant with raw water from a coastal aquifer for agricultural irrigation, Desalination and Water Treatment 31 (1-3) (2011) 331–338. doi:https://doi.org/10.5004/dwt.2011.2380.

[13] D. Zarzo, E. Campos, P. Terrero, Spanish experience in desalination for agriculture, Desalination and Water Treatment 51 (1-3) (2013) 53–66. doi:10.1080/19443994.2012.708155.

[14] B. Cohen, N. Lazarovitch, J. Gilron, Upgrading groundwater for irrigation using monovalent selective electrodialysis, Desalination 431 (2018) 126 – 139.
URL https://doi.org/10.1016/j.desal.2017.10.030

[15] E. Jones, M. Qadir, M. T. van Vliet, V. Smakhtin, S. mu Kang, The state of desalination and brine production: A global outlook, Science of The Total Environment 657 (2019) 1343–1356.
URL https://doi.org/10.1016/j.scitotenv.2018.12.076

[16] H. Strathmann, Electrodialysis, a mature technology with a multitude of new applications, Desalination 264 (3) (2010) 268 – 288.
URL https://doi.org/10.1016/j.desal.2010.04.069

[17] Y. D. Ahdab, D. Rehman, J. H. Lienhard, Brackish water desalination for greenhouses: Improving groundwater quality for irrigation using monovalent selective electrodialysis reversal, Journal of Membrane Science 610 (2020) 118072.
URL https://doi.org/10.1016/j.memsci.2020.118072

[18] Y. D. Ahdab, J. H. Lienhard, Desalination of brackish groundwater to improve water quality and water supply, in: Global Groundwater: Source, Scarcity, Sustainability, Security and Solutions, 1st Edition, Elsevier, 2020, ISBN 9780128181720.

[19] G. Doornbusch, M. van der Wal, M. Tedesco, J. Post, K. Nijmeijer, Z. Borneman, Multistage electrodialysis for desalination of natural seawater, Desalination 505 (2021) 114973.
URL https://doi.org/10.1016/j.desal.2021.114973

[20] K. G. Nayar, J. Fernandes, R. K. McGovern, K. P. Dominguez, A. McCance, B. S. Al-Anzi, J. H. Lienhard, Cost and energy requirements of hybrid RO and ED brine concentration systems for salt production, Desalination 456 (2019) 97 – 120. doi:https://doi.org/10.1016/j.desal.2018.11.018.
URL http://www.sciencedirect.com/science/article/pii/S0011916418312761

[21] M. Turek, Cost effective electrodialytic seawater desalination, Desalination 153 (1) (2003) 371–376. doi:https://doi.org/10.1016/S0011-9164(02)01130-X.
URL https://www.sciencedirect.com/science/article/pii/S001191640201130X

[22] M. Turek, Electrodialytic desalination and concentration of coal-mine brine, Desalination 162 (2004) 355–359.
URL https://doi.org/10.1016/S0011-9164(04)00069-4

[23] N. Kress, Chapter 2 - desalination technologies, in: N. Kress (Ed.), Marine Impacts of Seawater Desalination, Elsevier, 2019, pp. 11–34.
URL https://doi.org/10.1016/B978-0-12-811953-2.00002-5

[24] C.-S. Karavas, K. G. Arvanitis, G. Kyriakarakos, D. D. Piromalis, G. Papadakis, A novel autonomous pv powered desalination system based on a dc microgrid concept incorporating short-term energy storage, Solar Energy 159 (2018) 947–961.
URL https://doi.org/10.1016/j.solener.2017.11.057

[25] M. Isaka, Water desalination using renewable energy, Tech. rep., International Renewable Energy Agency (2013).
URL http://iea-etsap.org/E-TechDS/PDF/I12IR_Desalin_MI_Jan2013_final_GSOK.pdf

[26] K. G. Nayar, J. H. Lienhard, Brackish water desalination for greenhouse agriculture: Comparing the costs of RO, CCRO, EDR, and monovalent-selective EDR, Desalination 475 (2020) 114188.
URL https://doi.org/10.1016/j.desal.2019.114188

[27] G. Saracco, M. C. Zanetti, Ion transport through monovalent-anion-permselective membranes,

Industrial & Engineering Chemistry Research 33 (1) (1994) 96–101.
URL https://doi.org/10.1021/ie00025a013

[28] G. Saracco, Transport properties of monovalent-ion-permselective membranes, Chemical Engineering Science 52 (17) (1997) 3019–3031.
URL https://doi.org/10.1016/S0009-2509(97)00107-3

[29] T. Luo, S. Abdu, M. Wessling, Selectivity of ion exchange membranes: A review, Journal of Membrane Science 555 (2018) 429–454.
URL https://doi.org/10.1016/j.memsci.2018.03.051

[30] A. Gonzalez, M. Grágeda, S. Ushak, Assessment of pilot-scale water purification module with electrodialysis technology and solar energy, Applied Energy 206 (2017) 1643 – 1652. doi:https://doi.org/10.1016/j.apenergy.2017.09.101.
URL http://www.sciencedirect.com/science/article/pii/S0306261917313831

[31] W. Li, W. B. Krantz, E. R. Cornelissen, J. W. Post, A. R. Verliefde, C. Y. Tang, A novel hybrid process of reverse electrodialysis and reverse osmosis for low energy seawater desalination and brine management, Applied Energy 104 (2013) 592 – 602. doi:https://doi.org/10.1016/j.apenergy.2012.11.064.
URL http://www.sciencedirect.com/science/article/pii/S0306261912008690

[32] R. A. Tufa, Y. Noviello, G. Di Profio, F. Macedonio, A. Ali, E. Drioli, E. Fontananova, K. Bouzek, E. Curcio, Integrated membrane distillation-reverse electrodialysis system for energy-efficient seawater desalination, Applied Energy 253 (2019) 113551. doi:https://doi.org/10.1016/j.apenergy.2019.113551.
URL http://www.sciencedirect.com/science/article/pii/S0306261919312255

[33] R. K. McGovern, S. M. Zubair, J. H. Lienhard, The cost effectiveness of electrodialysis for diverse salinity applications, Desalination 348 (2014) 57–65. doi:https://doi.org/10.1016/j.desal.2014.06.010.
URL http://www.sciencedirect.com/science/article/pii/S0011916414003312

[34] Y. D. Ahdab, D. Rehman, G. Schücking, M. Barbosa, J. H. Lienhard, Treating irrigation water using high-performance membranes for monovalent selective electrodialysis, ACS ES&T Water. (2020). doi:10.1021/acsestwater.0c00012.

[35] W. Jiang, L. Lin, X. Xu, H. Wang, P. Xu, Physicochemical and electrochemical characterization of cation-exchange membranes modified with polyethyleneimine for elucidating enhanced monovalent permselectivity of electrodialysis, Journal of Membrane Science 572 (2019) 545–556.
URL https://doi.org/10.1016/j.memsci.2018.11.038

[36] D. Rehman, Y. D. Ahdab, J. H. Lienhard, Monovalent selective electrodialysis: Modelling multi-ionic transport across selective membranes, Water Research 199 (2021) 117171.
URL https://doi.org/10.1016/j.watres.2021.117171

[37] J. A. Cotruvo, Desalination guidelines development for drinking water: Background, Tech. rep., World Health Organization (8 2004).
URL https://www.who.int/water_sanitation_health/dwq/nutrientschap2.pdf

[38] ASTOM Corporation, Ion exchange membrane, accessed June 12, 2020 (2013).
URL http://www.astom-corp.jp/en/product/10.html

[39] B. Cobban, K. Faller, Electrodialysis and electrodialysis reversal: M38, Vol. 38, American Water Works Association, 1995.
URL http://arco-hvac.ir/wp-content/uploads/2018/04/AWWA_M38_Electrodialysis_and_Electrodialysis.pdf

[40] E. T. Sajtar, D. M. Bagley, Electrodialysis reversal: Process and cost approximations for treating coal-bed methane waters, Desalination and Water Treatment 2 (1-3) (2009) 284–294. arXiv:https://doi.org/10.5004/dwt.2009.259, doi:10.5004/dwt.2009.259.
URL https://doi.org/10.5004/dwt.2009.259

[41] R. K. McGovern, S. M. Zubair, J. H. Lienhard V, The benefits of hybridising electrodialysis with reverse osmosis, Journal of Membrane Science 469 (2014) 326 – 335. doi:https://doi.org/10.1016/j.memsci.2014.06.040.
URL http://www.sciencedirect.com/science/article/pii/S0376738814004918

[42] Ameridia Innovative Solutions, Inc., Daniel Bar, Personal communication to Yvana Ahdab, accessed June 15, 2019 (2019).
URL http://www.eurodia.com/index.php/en/the-eurodia-group

[43] Ameridia Innovative Solutions, Inc., Daniel Bar, Personal communication to Yvana Ahdab,

accessed December 21, 2020 (2020).
URL http://www.eurodia.com/index.php/en/the-eurodia-group

[44] FUJIFILM Manufacturing Europe B.V., Jeroen van Nunen, Personal communication to Yvana Ahdab, accessed June 15, 2019 (2020).
URL https://www.fujifilmmembranes.com/

[45] T. Tetreault, SBA loan rates 2019 – current interest rates and how they work, accessed Jan 10, 2020 (2019).
URL https://fitsmallbusiness.com/sba-loan-rates/

[46] K. G. Nayar, J. H. Lienhard, Brackish water desalination for greenhouse agriculture: Comparing the costs of RO, CCRO, EDR, and monovalent-selective EDR, Desalination 475 (2020) 114188. doi:https://doi.org/10.1016/j.desal.2019.114188.

[47] E. Vartiainen, G. Masson, C. Breyer, D. Moser, E. Román Medina, Impact of weighted average cost of capital, capital expenditure, and other parameters on future utility-scale pv levelised cost of electricity, Progress in Photovoltaics: Research and Applications 28 (6) (2020) 439–453. doi:https://doi.org/10.1002/pip.3189.

[48] C. Kost, S. Shammugam, V. Julch, H.-T. Nguyen, T. Schlegl, Levelized cost of electricity renewable energy technologies, Tech. rep., Fraunhofer Institute for Solar Energy Systems ISE (2018).
URL https://www.connaissancedesenergies.org/sites/default/files/pdf-actualites/en2018_fraunhofer-ise_lcoe_renewable_energy_technologies.pdf

[49] M. Suri, Energy yield assessment of the photovoltaic power plant, Tech. rep., Solargis (2016).
URL https://solargis2-web-assets.s3.eu-west-1.amazonaws.com/public/sample/48a9f2ada0/Solargis-PVrep-200-01-2013-DEMO-v0b.pdf

[50] Solar resource and photovoltaic potential of Indonesia, Tech. rep., The World Bank (2017).
URL http://documents1.worldbank.org/curated/en/729411496240730378/pdf/115347-ESM-P145273-PUBLIC-IndonesiaSolarResourcePotentialWBESMAPMay.pdf

[51] M. Kettani, P. Bandelier, Techno-economic assessment of solar energy coupling with large-scale desalination plant: The case of morocco, Desalination 494 (2020) 114627.
URL https://doi.org/10.1016/j.desal.2020.114627

[52] G. M. Gold, M. E. Webber, The energy-water nexus: an analysis and comparison of various configurations integrating desalination with renewable power, Resources 4 (2) (2015) 227–276. URL https://doi.org/10.3390/resources4020227

[53] SUEZ Water Technologies & Solutions, Neil Moe, Personal communication to Yvana Ahdab, accessed December 8, 2020 (2020).
URL https://www.suezwatertechnologies.com/

[54] A. Panagopoulos, K.-J. Haralambous, M. Loizidou, Desalination brine disposal methods and treatment technologies - a review, Science of The Total Environment 693 (2019) 133545. doi:https://doi.org/10.1016/j.scitotenv.2019.07.351.
URL http://www.sciencedirect.com/science/article/pii/S0048969719334655

[55] K. M. Chehayeb, K. G. Nayar, J. H. Lienhard, On the merits of using multi-stage and counterflow electrodialysis for reduced energy consumption, Desalination 439 (2018) 1–16. doi:https://doi.org/10.1016/j.desal.2018.03.026.

[56] M. Turek, Dual-purpose desalination-salt production electrodialysis, Desalination 153 (1-3) (2003) 377–381. doi:https://doi.org/10.1016/S0011-9164(02)01131-1.

[57] N. Voutchkov, Desalination Project Cost Estimating and Management, CRC Press, 2019. doi:10.1201/9781351242738.

[58] J. E. Miller, Review of water resources and desalination technologies, Sandia National Laboratories, Albuquerque, NM 49 (2003) 2003–0800. doi:10.2172/809106.

[59] Y. D. Ahdab, J. H. Lienhard, Desalination of brackish groundwater to improve water quality and water supply, in: A. Mukherjee, B. R. Scanlon, A. Aureli, S. Langan, H. Guo, A. A. McKenzie (Eds.), Global Groundwater, Elsevier, 2021, pp. 559 – 575. doi:https://doi.org/10.1016/B978-0-12-818172-0.00041-4.
URL http://www.sciencedirect.com/science/article/pii/B9780128181720000414

[60] Clemson University Agricultural Service Laboratory, Fertility recommendations: Small area (square footage) (2019).
URL https://www.clemson.edu/public/regulatory/ag-srvc-lab/soil-testing/recommendations.html

[61] Agvise Laboratories, Soil amendments (2019).
URL https://www.agvise.com/agronomic-information/educational-articles/

[62] Alpha chemicals, Product: Calcium sulfate dihydrate - $CaSO_4 * 2H_2O$, accessed July 17, 2019.
URL https://alphachemicals.com/calcium_sulfate

[63] PowerGrow Systems, Product: Epsom salt (magnesium sulfate) - agricultural grade, accessed July 17, 2019.
URL https://www.powergrowsystems.com/products/epsom-salt-magnesium-sulfate-agricultural-grade?variant=40175466190

[64] E. Will, J. E. Faust, Irrigation water quality for greenhouse production, Agricultural Extension Service, The University of Tennessee (1999).
URL http://trace.tennessee.edu/utk_agexcomhort/5

[65] P. Dlugolkecki, B. Anet, S. J. Metz, K. Nijmeijer, M. Wessling, Transport limitations in ion exchange membranes at low salt concentrations, Journal of Membrane Science 346 (1) (2010) 163–171.
URL https://doi.org/10.1016/j.memsci.2009.09.033

[66] H. Strathmann, Ion-exchange membrane separation processes, Vol. 9, Elsevier B.V., Amsterdam, The Netherlands, 2004.

[67] L. Firdaous, J. Malériat, J. Schlumpf, F. Quéméneur, Transfer of monovalent and divalent cations in salt solutions by electrodialysis, Separation Science and Technology 42 (5) (2007) 931–948. arXiv:https://doi.org/10.1080/01496390701206413, doi:10.1080/01496390701206413.
URL https://doi.org/10.1080/01496390701206413

[68] J. Burgess, Ions in Solution, Woodhead Publishing, Cambridge, England, 1999. doi:10.1533/9781782420569.45.

[69] T. Luo, Aqueduct Global Maps 3.0, Dataset used for visualization (2020).
URL https://www.wri.org/resources/data-sets/aqueduct-global-maps-30-data

[70] Energy Sector Management Assistance Program, Global Solar Atlas 2.0, Dataset used for visualization (2019).
URL https://globalsolaratlas.info/map?c=11.609193,8.261719,3

[71] Australia electricity prices [online] (March 2020) [cited 9 December 2020].

[72] A. Vagneur-Jones, D. Traum, Sub-Saharan Africa Market Outlook 2020, Tech. rep., Bloomberg Finance L.P. (February 2020).
URL https://global-climatescope.org/assets/data/docs/updates/2020-02-06-sub-saharan-africa-market-outlook-2020.pdf

[73] M. M. (Bloomberg), Solar electricity can retail for $0.027–0.036/kwh as renewables close in on global grid parity (2019).
URL https://www.pv-magazine.com/2019/11/01/solar-electricity-can-retail-for-0-027-0-036-kwh-as-renewables-close-in-on-global-grid-parity/

[74] U.S. Energy Information Administration. Electricity data browser [online, cited 9 December 2020].

[75] B. Neff, Estimated cost of new utility-scale generation in California: 2018 update, Tech. Rep. CEC-200-2019-500, California Energy Commission (2019).
URL https://ww2.energy.ca.gov/2019publications/CEC-200-2019-005/

[76] International Energy Agency, Key World Energy Statistics 2020, Statistics report (August 2020).
URL https://www.iea.org/reports/key-world-energy-statistics-2020

[77] E. C. Board, ESI Statistical Bulletin 2016: Electricity Access in Namibia (2017).
URL https://www.ecb.org.na/images/docs/Statistical_Bulletin/ESI_Stats_Bulletin_2016.pdf

[78] Clean Energy Business Council, Energy efficiency white paper (January 2018).
URL https://cebcmena.com/whatwedo/gcc-energy-consumption/

[79] D. D. (Forbes), Race heats up for title of cheapest solar energy in the world (2019).
URL https://www.forbes.com/sites/dominicdudley/2019/10/17/cheapest-solar-energy-in-the-world/#1a1418c34772

[80] The Straits Times, Pub seeks to cut energy need for desalination (2018).
URL https://www.straitstimes.com/singapore/pub-seeks-to-cut-energy-needed-for-desalination

[81] D. A. Cowan, J. H. Brown, Effect of turbulence on limiting current in electrodialysis cells, Industrial & Engineering Chemistry 51 (12) (1959) 1445–1448.
URL https://doi.org/10.1021/ie50600a026

[82] Global Water Intelligence, Desaldata cost estimator (2020).
URL https://www.desaldata.com/cost_estimator

[83] E. Coutinho de Paula, M. C. S. Amaral, Extending the life-cycle of reverse osmosis membranes: A review, Waste Management & Research 35 (5) (2017) 456–470. doi:https://doi.org/10.1177/0734242X16684383.